Investigation of limit cycles and signal stabilization of two dimensional systems with memory type nonlinear elements

K.C. PATRA and B.K. DAKUA

The paper presents a simple, systematic and novel graphical method which uses computer graphics for prediction of limit cycles in two dimensional multivariable nonlinear system having rectangular hysteresis and backlash type nonlinearities. It also explores the avoidance of such self-sustained oscillations by determining the stability boundary of the system. The stability boundary is obtained using simple Routh Hurwitz criterion and the incremental input describing function, developed from harmonic balance concept. This may be useful in interconnected power system which utilizes governor control. If the avoidance of limit cycle or a safer operating zone is not possible, the quenching of such oscillations may be done by using the signal stabilization technique which is also described. The synchronization boundary is laid down in the forcing signal amplitudes plane using digital simulation. Results of digital simulations illustrate accuracy of the method for 2×2 systems.

Key words: describing function, dither signal, incremental input describing function, limit cycles, signal stabilization, stability boundary

A.   Introduction

Growing interest in prediction of limit cycles in 2×2 nonlinear systems has been closely noticed among researchers for several decades [1–18]. The problem is remarkable and more complex in the presence of memory type nonlinearity [8, 19, 24, 34–36]. The situation is worse because literature seldom discusses methods of quenching the limit cycle oscillations sustained in the system under autonomous state [17, 24].

It has been realized that the exhibition of limit cycle in two dimensional multivariable nonlinear systems in several occasions like Couple Core Reactor [29],

The Authors are with the Department of Electrical Engineering, C.V. Raman College of Engineering, Bhubaneswar, Odisha (INDIA) 752054.

K.C. Patra is the corresponding author. Tel.: +91 94370 87770; E-mails: kcpatra47@rediffmail / kcpatra47@gmail.com; Orcid ID: 0000-0002-4693-4883.

PWR Nuclear reactor systems [18], radar antenna pointing system [16] and Interconnected Power System [32] which can fit the structure [25] of a general two dimensional nonlinear system, has been addressed in the present work.

Existing practice of power system, interconnected with various areas through tie-lines, sometimes suffers from mismatches in frequency because of area load change and also some other abnormal conditions. The popular, the simple, easy realisation, low cost, robust and decentralised nature of the control strategy, the load frequency control (LFC) is used immensely. The LFC also shows poor performance for the presence of backlash nonlinearities in the Governors [32]. It has been stressed on the LFC scheme in the zone of operation avoiding the existence of Limit Cycle or reducing the amplitude of sustaining oscillations. It may not be always possible to have such safer zone of operation i.e. either absence of limit cycle or reduction in amplitude of self sustained oscillations.

In some recent literature [36] the limit cycle induced by backlash nonlinearity is discussed, but detailed analysis, well established conclusions and straight forward techniques are still lacking [30]. The suppression of limit cycle oscillation using state feedback approach has been dealt to an extent [36]. Investigation has also been done to find the existence of limit cycle oscillations in combustion chambers of gas turbines [8] and for a combustor with long flame [11] which are different from the general stream unlike the present work. In some cases like [7] prediction of limit cycle under uncertainty has been discussed.

The present work proposes harmonic balance concept leading to a graphical method has been adopted for prediction of limit cycles in 2×2 general systems with rectangular hysteresis and backlash type nonlinearities which claim to be the novel method for memory type nonlinearities not been detailed elsewhere. The possibility of quenching the limit cycle considering the method of signal stabilization has also been investigated [17, 20, 21, 24]. In sequel the stabilization boundary [21] of the system is determined. All such developments either by graphical or analytical approach have been substantiated by digital simulation or with the use of MATLAB/SIMULINK application.

B.   Prediction of limit cycle in a class of 2×2 systems with memory type nonlinearities

B.1.   Rectangular hysteresis

B.1.1.   Graphical method

Consider a system having two interconnected subsystems as given in Fig. 1, which represents a class of general 2×2 systems [25, 26]. In the system N_1, N_2 are two nonlinear elements with Rectangular Hysteresis input-output characteristics as shown in Fig. 2a and 2b, respectively. G_1, G_2 are two linear elements.
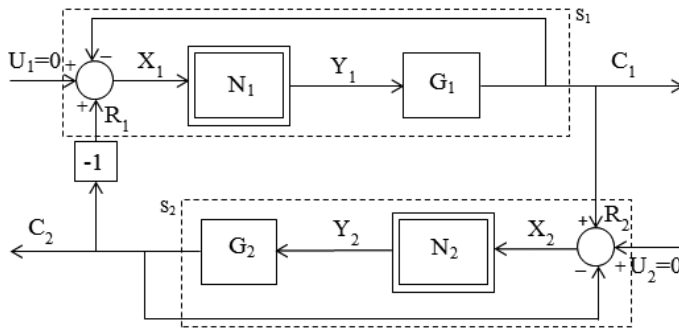
www.czasopisma.pan.pl   PAN   www.journals.pan.pl

POLSKA AKADEMIA NAUK

INVESTIGATION OF LIMIT CYCLES AND SIGNAL STABILIZATION
OF TWO DIMENSIONAL SYSTEMS WITH MEMORY TYPE NONLINEAR ELEMENTS   287

Figure 1: A class of 2×2 nonlinear system

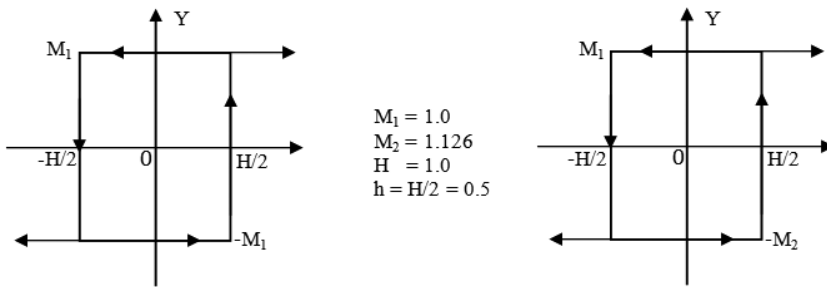

$M_1 = 1.0$
$M_2 = 1.126$
$H = 1.0$
$h = H/2 = 0.5$

Figure 2: Input-output characteristics of nonlinear elements N_1 and N_2
(Rectangular Hysteresis type nonlinearities)

The simpler analysis is possible with the assumptions that the system exhibits
self oscillation at a single frequency and the loop possesses low pass character-
istics. Harmonic balance method is used to develop a graphical technique in the
following lines.

The describing function for the rectangular hysteresis nonlinearity is ex-
pressed as:

$$N(X,\omega) = \frac{Y}{X} \angle \theta = \begin{cases} 0, & X < \dfrac{H}{2}, \\[2ex] \dfrac{4M}{\pi X} \angle - \sin^{-1} \dfrac{H}{2X}, & X > \dfrac{H}{2}. \end{cases}$$

When the system exhibits limit cycle the phasor diagram can be drawn as in
Fig. 3a and subsequently the normalized phasor diagram with respect to R_1 is
shown as in Fig. 3b. The determination of different quantities through graphical
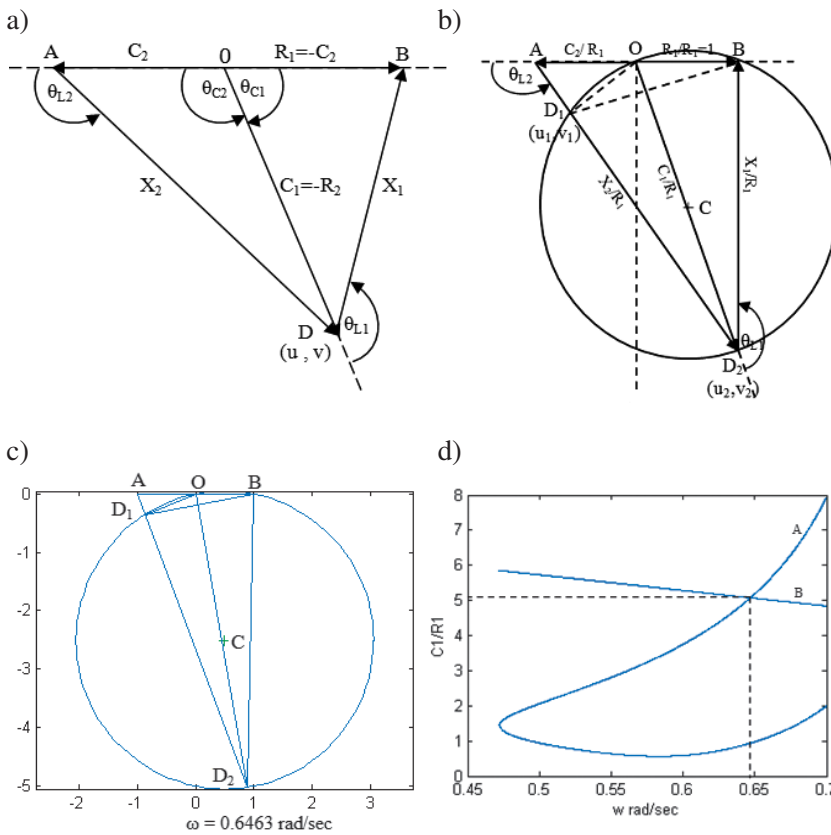procedure is illustrated through examples.

a)

b)

c)

d)

Figure 3: a) phasor diagram for a 2×2 nonlinear system; b) normalised phasor diagram for a simplified generalised 2×2 nonlinear system; c) normalised phasor diagram for example 1 with $\omega = 0.6463$ rad/sec; d) solution of the system in Example 1

Example 1

Consider the system of Fig. 1 with the linear elements:

$$G_1(s) = \frac{2}{s(s+1)^2}, \qquad G_2(s) = \frac{1}{s(s+4)},$$

whereas the nonlinear elements are shown as in Fig. 2a and 2b where $h = \dfrac{H}{2}$.

Memory type nonlinearities contribute additional phase angle to the loop phase angles of $G_1(j\omega)$ and $G_2(j\omega)$ of subsystem (1) and (2) respectively which are taken care of in the respective methods of prediction of limit cycles as well as in the signal stabilizations.

For subsystem (1)

$$\theta_{L_1} = \theta_{N_1(X_1,\omega)} + \theta_{G_1(j\omega)}$$

www.czasopisma.pan.pl   PAN   www.journals.pan.pl

POLSKA AKADEMIA NAUK

INVESTIGATION OF LIMIT CYCLES AND SIGNAL STABILIZATION
OF TWO DIMENSIONAL SYSTEMS WITH MEMORY TYPE NONLINEAR ELEMENTS   289

$$\theta_{L_1} = -\sin^{-1}\frac{H}{2X_1} - \frac{\pi}{2} - 2\tan^{-1}\omega. \tag{1}$$

For subsystem (2)

$$\theta_{L_2} = \theta_{N_2(X_2,\omega)} + \theta_{G_2(j\omega)}$$

or

$$\theta_{L_2} = -\sin^{-1}\frac{H}{2X_2} - \frac{\pi}{2} - \tan^{-1}\frac{\omega}{4}. \tag{2}$$

In graphical method [26], while θ_{L_1} traces a circle, θ_{L_2} traces a straight line. Radius of the above mentioned circle is: $r = \dfrac{1}{2\sin\theta_{L_1}}$ and centre of the circle is at

$$\left(0.5, \frac{-1}{2\tan\theta_{L_1}}\right) \tag{3}$$

The point of intersection of the circle and the straight line is at (u_i, v_i), which can be obtained as follows:

$$u_i = \frac{v_i}{\tan\theta_{L_2}} - 1 \tag{4}$$

and

$$v_i = \frac{3\cot\theta_{L_2} + \cot\theta_{L_1} \pm \sqrt{(3\cot\theta_{L_2} + \cot\theta_{L_1})^2 - 8\csc^2\theta_{L_2}}}{2\csc^2\theta_{L_2}}. \tag{5}$$

The phasor diagram of the above system can be obtained by using the following relationship (cf. Eq. (6)) shown in Fig. 3a and the normalised one shown in Fig. 3b.

$$R_1 = X_1 + C_1, \quad R_2 = X_2 + C_2, \quad R_2 = C_1, \quad R_1 = -C_2. \tag{6}$$

Again from the above mentioned system

$$\frac{C_1}{R_1} = \frac{M_1}{M_2} = \frac{G_1}{G_2} = 1.7762\frac{\sqrt{16+\omega^2}}{1+\omega^2}, \tag{7}$$

where, $M_1 = 1.0$, $M_2 = 1.126$ and C_1, C_2, R_1, R_2, X_1, X_2 are amplitudes of respective sinusoids and G_1, G_2 are magnitudes or absolute values of the respective transfer functions.

Fig. 3c shows the graphical determinations of different quantities utilising the data from Table 1. The values of $\dfrac{C_1}{R_1}$ for different values of ω are calculated from Eq. (7) as well as from the graphical plot of figures (cf. Fig. 3c). The point of intersection of these two curves provides the frequency of the limit cycle of Example 1.

Table 1: Values of different quantities for Example 1

ω	θ_{L_1}	θ_{L_2}	$\dfrac{C_1}{R_1}$ from plot	$\dfrac{C_1}{R_1}$ from Eq. (6)
0.60	-164.82	-109.83	0.58, 3.76	5.28
0.61	-165.66	-109.97	0.62, 3.99	5.23
0.62	-166.49	-110.11	0.68, 4.25	5.19
0.63	-167.31	-110.25	0.76, 4.54	5.14
0.64	-168.13	-110.39	0.86, 4.85	5.10
0.6463	-168.64	-110.48	0.93, **5.07**	**5.07 (LC)**
0.65	-168.94	-110.53	0.98, 5.21	5.06
0.70	-172.88	-111.23	2.02, 8.00	4.87

Fig. 3d shows the variation of $\dfrac{C_1}{R_1}$ from the phasor diagram (curve A) and from Eq. (7) (curve B) for different values of frequency ω (cf. Table 1).

The point of the intersection of curve (A) and curve (B) provides the value of limit cycle frequency $\omega = 0.6463$ rad/sec.

Again, corresponding to this value of ω,

$$\frac{C_1}{R_1} = 5.0782, \qquad \frac{X_1}{R_1} = 5.0049,$$
$$\frac{C_2}{R_1} = 1.0, \qquad \frac{X_2}{R_1} = 5.3410.$$

This provides the parameter of the limit cycle as:

$$X_1 = \frac{4M_1G_1}{\pi}\left(\frac{BD}{OD}\right) = 2.7291,$$
$$X_2 = \frac{4M_2G_2}{\pi}\left(\frac{AD}{OA}\right) = 2.9240,$$
$$C_1 = 2.7792, \qquad C_2 = 0.5472.$$

B.1.2. Digital simulation

Example 1 is revisited, as shown in Fig. 4a. Following the procedure as outlined in [23], the limit cycle is predicted using the digital simulation technique.

$$G_1(s) = \frac{2}{s(s+1)^2} = \frac{2}{s} - \frac{2}{(s+1)^2} - \frac{2}{s+1}, \qquad (8)$$

www.czasopisma.pan.pl   PAN   www.journals.pan.pl

POLSKA AKADEMIA NAUK

INVESTIGATION OF LIMIT CYCLES AND SIGNAL STABILIZATION
OF TWO DIMENSIONAL SYSTEMS WITH MEMORY TYPE NONLINEAR ELEMENTS   291

$$G_2(s) = \frac{1}{s(s+4)} = \frac{0.25}{s} - \frac{0.25}{s+4}. \tag{9}$$

For very small value of the sampling period (T)
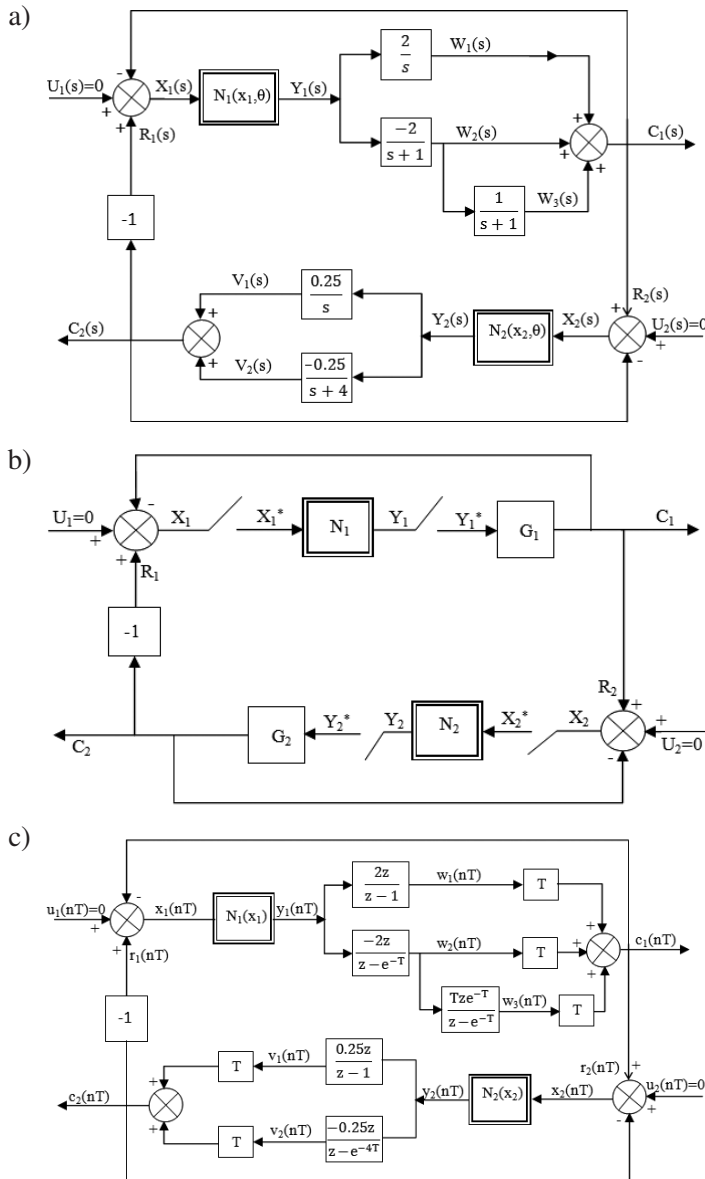
$$TG(z) \simeq G(s).$$

Figure 4: Digital simulation of the system in Example 1: a) canonical representation of
the system, b) equivalent sample data system, c) digital representation in Z-domain

Hence, inserting the sampling period (T) as gain and taking the Z-transform of the above functions, Fig. 4a can be equivalently represented in sampled data form and digital form in z domain as Fig. 4b and Fig. 4c respectively. This procedure yields:

$$y_1(nT) = f_1 x_1(nT),$$
$$y_2(nT) = f_2 x_2(nT),$$
$$x_1(nT) = r_1(nT) - c_1(nT),$$
$$x_2(nT) = r_2(nT) - c_2(nT),$$
$$r_1(nT) = -c_2(nT),$$
$$r_2(nT) = c_1(nT).$$

As $\dfrac{W_1(s)}{Y_1(s)} = \dfrac{2}{s}$, taking Z-transform

$$\frac{W_1(z)}{Y_1(z)} = 2\left(\frac{z}{z-1}\right) = \frac{2}{1-z^{-1}},$$

$$W_1(z)(1-z^{-1}) = 2Y_1(z),$$
$$W_1(z) - z^{-1}W_1(z) = 2Y_1(z)$$

or

$$W_1(z) = 2Y_1(z) + z^{-1}W_1(z).$$

Taking inverse Z-transform,

$$w_1(nT) = 2y_1(nT) + w_1[(n-1)T]. \tag{10}$$

Again

$$\frac{W_2(s)}{Y_1(s)} = \frac{-2}{s+1} \quad \text{or} \quad \frac{W_2(z)}{Y_1(z)} = \frac{-2z}{z-e^{-T}} = \frac{-2}{1-z^{-1}e^{-T}}.$$

Hence

$$W_2(z)(1-z^{-1}e^{-T}) = -2Y_1(z) \quad \text{or} \quad W_2(z) = -2Y_1(z) + z^{-1}e^{-T}W_2(z).$$

Taking inverse Z-transform,

$$w_2(nT) = -2y_1(nT) + e^{-T}w_2[(n-1)T]. \tag{11}$$

Further

$$\frac{W_3(s)}{W_2(s)} = \frac{1}{s+1} \quad \text{or} \quad \frac{W_3(z)}{W_2(z)} = \frac{Tze^{-T}}{z-e^{-T}} = \frac{Te^{-T}}{1-z^{-1}e^{-T}},$$

www.czasopisma.pan.pl   PAN   www.journals.pan.pl
POLSKA AKADEMIA NAUK

INVESTIGATION OF LIMIT CYCLES AND SIGNAL STABILIZATION
OF TWO DIMENSIONAL SYSTEMS WITH MEMORY TYPE NONLINEAR ELEMENTS   293

$$W_3(z)(1 - z^{-1}e^{-T}) = W_2(z)(Te^{-T})$$

or

$$W_3(z) = (Te^{-T})W_2(z) + (z^{-1}e^{-T})W_3(z).$$

Taking inverse Z-transform,

$$w_3(nT) = Te^{-T}w_2(nT) + e^{-T}w_3[(n-1)T]. \tag{12}$$

Similarly,

$$\frac{V_1(s)}{Y_2(s)} = \frac{0.25}{s} \quad \text{or} \quad \frac{V_1(z)}{Y_2(z)} = \frac{0.25z}{z-1} = \frac{0.25}{1-z^{-1}},$$

$$V_1(z) - z^{-1}V_1(z) = 0.25Y_2(z) \quad \text{or} \quad V_1(z) = 0.25Y_2(z) + z^{-1}V_1(z).$$

Taking inverse Z-transform,

$$v_1(nT) = 0.25y_2(nT) + v_1[(n-1)T]. \tag{13}$$

Again,

$$\frac{V_2(s)}{Y_2(s)} = \frac{-0.25}{s+4} \quad \text{or} \quad \frac{V_2(z)}{Y_2(z)} = \frac{-0.25z}{z - e^{-4T}} = \frac{-0.25}{1 - z^{-1}e^{-4T}},$$

$$V_2(z) = -0.25Y_2(z) + z^{-1}e^{-4T}V_2(z).$$

Taking inverse Z-transform,

$$v_2(nT) = -0.25y_2(nT) + e^{-4T}v_2[(n-1)T]. \tag{14}$$

Since

$$TG(z) \simeq G(s).$$

Hence,

$$C_1(z) = T[W_1(z) + W_2(z) + W_3(z)].$$

Taking inverse Z-transform,

$$c_1(nT) = T[w_1(nT) + w_2(nT) + w_3(nT)]. \tag{15}$$

Again $C_2(z) = T[V_1(z) + V_2(z)]$, hence taking inverse Z-transform,

$$c_2(nT) = T[v_1(nT) + v_2(nT)]. \tag{16}$$

The results of digital simulation are shown in Fig. 5 and compared in Table 2 with the results obtained from the graphical method and also that of SIMULINK application.
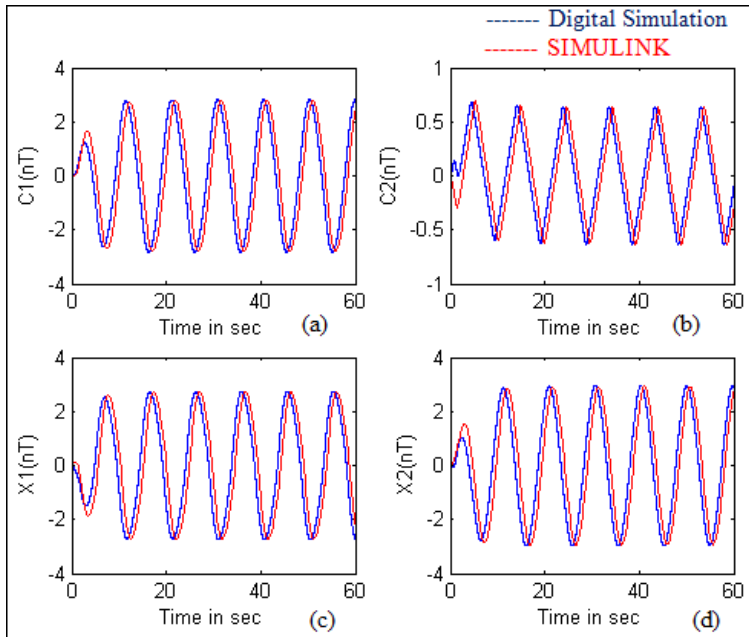
Figure 5: Results of Example 1 for C_1, C_2, X_1, and X_2 obtained from Digital Simulation and SIMULINK application

Table 2: Comparison of results of Example 1

Methods of Computation	ω (rad/sec)	X_1	X_2	C_1	C_2
Graphical	0.6463	2.73	2.92	2.77	0.54
Digital Simulation	0.6472	2.72	2.94	2.80	0.62
SIMULINK	0.6465	2.73	2.94	2.80	0.69

B.1.3. Simulation using MATLAB/SIMULINK

The above mentioned system of Example 1 of Fig. 1 is simulated using MAT-LAB/SIMULINK Toolbox. The result is shown in Fig. 5 and compared with that of graphical method and the digital simulation in Table 2.

B.2. Backlash nonlinearity

B.2.1. Graphical method

Consider a system of Fig. 1 where N_1 and N_2 are two nonlinear elements with backlash input-output characteristics as shown in Fig. 6. G_1, G_2 are the transfer functions of the linear elements.

www.czasopisma.pan.pl   PAN   www.journals.pan.pl
POLSKA AKADEMIA NAUK

INVESTIGATION OF LIMIT CYCLES AND SIGNAL STABILIZATION
OF TWO DIMENSIONAL SYSTEMS WITH MEMORY TYPE NONLINEAR ELEMENTS   295
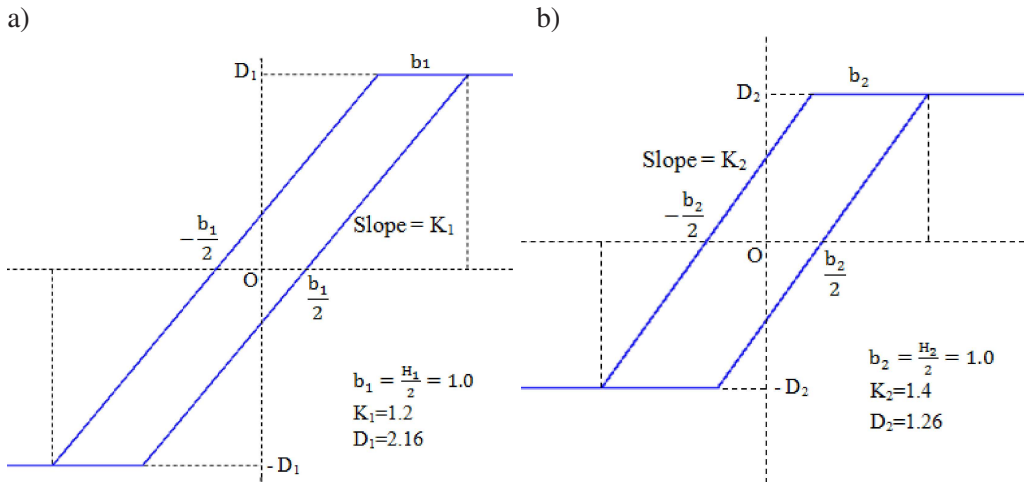
a)

b)

Figure 6: Input–output characteristic of nonlinear elements N_1 and N_2

The graphical method based on normalised phasor diagram [21, 26] is used for prediction of limit cycle in the system which has been illustrated through an example. The whole system is assumed to exhibit oscillation predominantly at a single frequency. Backlash nonlinearities contribute additional phase angle to the loop phase angles of $G_1(j\omega)$ and $G_2(j\omega)$ of the subsystems (1) and (2).

Example 2

Consider the system of Fig. 1 with $G_1(s) = \dfrac{2}{s(s+1)^2}$; $G_2(s) = \dfrac{2}{s(s+4)}$ and the two nonlinear elements having backlash characteristics with $b_1 = b_2 = 1.0$ as shown in Fig. 6.

Describing function of the above Backlash Nonlinearities is expressed as:

$$N(X_m, \omega) = \left| \frac{Y}{X_m} \angle \emptyset \right|$$

or

$$N(X_m, \omega) = \frac{\dfrac{KX_m}{\pi} \sqrt{\left(\dfrac{\pi}{2} + \beta + \dfrac{1}{2}\sin\beta\right)^2 + \cos^4\beta}}{X_m}$$

$$\angle - \tan^1 \left(\frac{\cos^2\beta}{\dfrac{\pi}{2} + \beta_1 + \dfrac{1}{2}\sin 2\beta} \right)$$

or

$$
N(X_m, \omega) = \begin{cases} \dfrac{\dfrac{K}{\pi}\sqrt{\left(\dfrac{\pi}{2}+\beta+\dfrac{1}{2}\sin 2\beta\right)^2+\cos^4\beta}}{X_m}\angle -\tan^1\left(\dfrac{\cos^2\beta}{\dfrac{\pi}{2}+\beta+\dfrac{1}{2}\sin 2\beta}\right) \\ \hspace{6cm} \text{for } X_m > \dfrac{b}{2}, \\[2mm] 0 \hspace{4.5cm} \text{for } X_m < \dfrac{b}{2} \end{cases} \tag{17}
$$

and

$$
N_1(X_{m1}, \omega) = \frac{K_1}{\pi}\sqrt{\left(\frac{\pi}{2}+\beta_1+\frac{1}{2}\sin 2\beta_1\right)^2+\cos^4\beta_1}.
$$

Again,

$$
N_2(X_{m2}, \omega) = \frac{K_2}{\pi}\sqrt{\left(\frac{\pi}{2}+\beta_2+\frac{1}{2}\sin 2\beta_2\right)^2+\cos^4\beta_2}.
$$

The detailed derivation is shown in Appendix A1.

The limit cycling condition of the system can be represented by the phasor diagram shown in Fig. 7a and subsequently the normalised phasor diagram in Fig. 7b.

For subsystem (1)

$$
\theta_{L_1} = \theta_{N_1(X_{m1}, \omega)} + \theta_{G_1(j\omega)}
$$

or

$$
\theta_{L_1} = \left[-\tan^{-1}\left(\frac{\cos^2\beta_1}{\dfrac{\pi}{2}+\beta_1+\dfrac{1}{2}\sin^2\beta_1}\right)\frac{-\pi}{2}-2\tan^{-1}\omega\right], \tag{18}
$$

where

$$
\beta_1 = \sin^{-1}\left(1-\frac{b_1}{X_{m1}}\right).
$$

Similarly

$$
\theta_{L_2} = \theta_{N_2(X_{m2}, \omega)} + \theta_{G_2(j\omega)}
$$

or

$$
\theta_{L_2} = \left[-\tan^{-1}\left(\frac{\cos^2\beta_2}{\dfrac{\pi}{2}+\beta_2+\dfrac{1}{2}\sin^2\beta_2}\right)\frac{-\pi}{2}-\tan^{-1}\left(\frac{\omega}{4}\right)\right], \tag{19}
$$

where

$$
\beta_2 = \sin^{-1}\left(1-\frac{b_2}{X_{m2}}\right).
$$

www.czasopisma.pan.pl   PAN   www.journals.pan.pl

POLSKA AKADEMIA NAUK

INVESTIGATION OF LIMIT CYCLES AND SIGNAL STABILIZATION
OF TWO DIMENSIONAL SYSTEMS WITH MEMORY TYPE NONLINEAR ELEMENTS   297
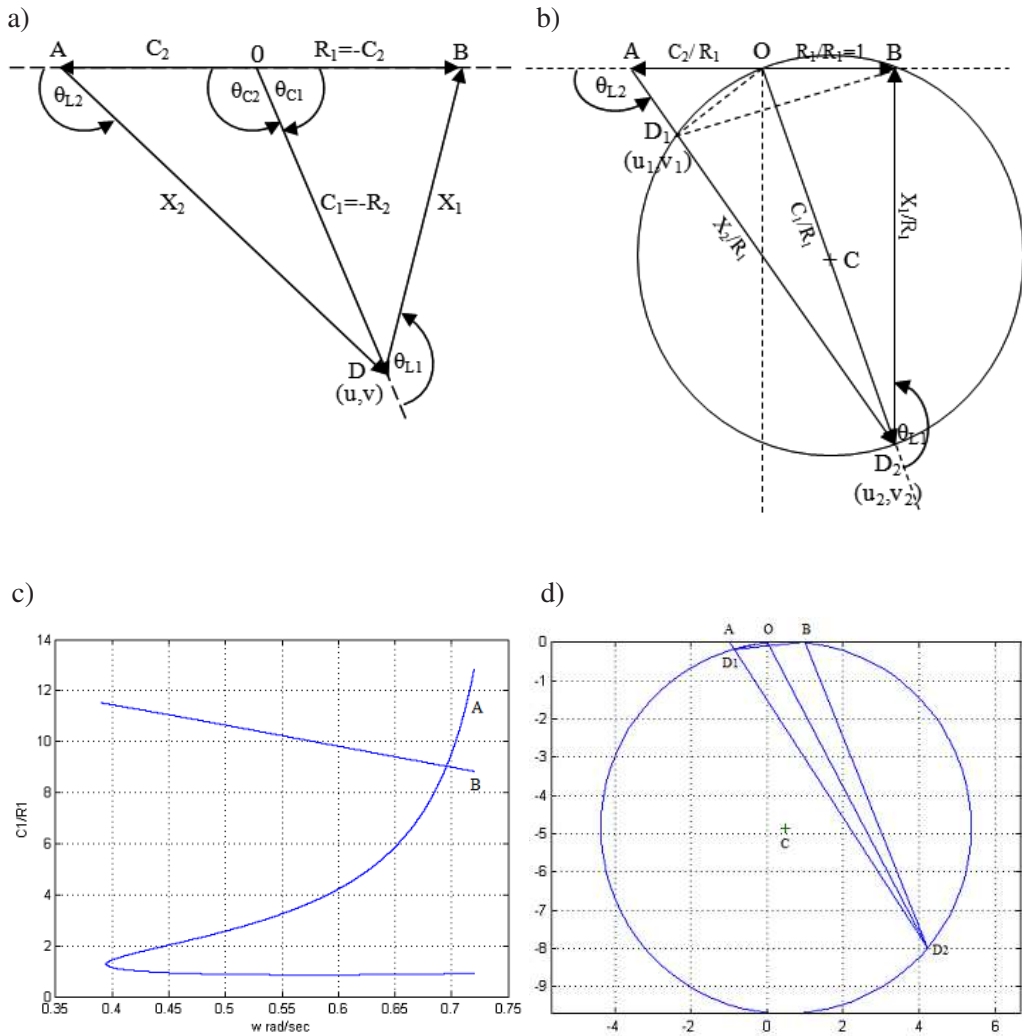

Figure 7: a) Phasor diagram for a 2×2 nonlinear system, b) normalised phasor diagram for a simplified generalised 2×2 nonlinear system, c) solution of the system in Example 2, d) normalised phasor diagram for Example 2 with $\omega = 0.6955$ rad/sec

In this case also Eqs. (3), (4), (5) and (6) are valid whereas:

$$\frac{C_1}{R_1} = \frac{C_1}{C_2} = \frac{Y_1 G_1}{Y_2 G_2} = \frac{X_{m1} N_1 G_1}{X_{m2} N_2 G_2}$$

or

$$\frac{C_1}{R_1} = \frac{(X_{m1}G_1)\dfrac{K_1}{\pi}\sqrt{\left(\dfrac{\pi}{2}+\beta_1+\dfrac{1}{2}\sin 2\beta_1\right)^2+\cos^4\beta_1}}{(X_{m2}G_2)\dfrac{K_2}{\pi}\sqrt{\left(\dfrac{\pi}{2}+\beta_2+\dfrac{1}{2}\sin 2\beta_2\right)^2+\cos^4\beta_2}},$$

$$\frac{C_1}{R_1} = \frac{K_1 X_{m1} G_1}{K_2 X_{m2} G_2}\frac{\sqrt{\left(\dfrac{\pi}{2}+\beta_1+\dfrac{1}{2}\sin 2\beta_1\right)^2+\cos^4\beta_1}}{\sqrt{\left(\dfrac{\pi}{2}+\beta_2+\dfrac{1}{2}\sin 2\beta_2\right)^2+\cos^4\beta_2}}, \quad (20)$$

$$K_1 = 1.2; \qquad K_2 = 1.4,$$

where, Y_1, Y_2, N_1, N_2, G_1 and G_2 are magnitude or absolute values of the respective transfer functions.

Since

$$|G_1(j\omega)| = \frac{2}{\omega(1+\omega^2)}; \qquad |G_2(j\omega)| = \frac{1}{\omega\sqrt{16+\omega^2}},$$

$$\left|\frac{G_1}{G_2}\right| = \frac{\dfrac{2}{\omega(1+\omega^2)}}{\dfrac{1}{\omega\sqrt{16+\omega^2}}} = \frac{2\sqrt{16+\omega^2}}{(1+\omega^2)}.$$

Eq. (20) can be written as:

$$\frac{C_1}{R_1} = \frac{1.714\times 1\sqrt{16+\omega^2}}{X_{m2}(1+\omega^2)}\frac{\sqrt{\left(\dfrac{\pi}{2}+\beta_1+\dfrac{1}{2}\sin 2\beta_1\right)^2+\cos^4\beta_1}}{\sqrt{\left(\dfrac{\pi}{2}+\beta_2+\dfrac{1}{2}\sin 2\beta_2\right)^2+\cos^4\beta_2}}. \quad (21)$$

Several normalised phasor diagrams are drawn to scale utilizing the data from Table 3. The values of $\dfrac{C_1}{R_1}$ for different values of ω are calculated using Eq. (21) as well as from the graphical plots (cf. Fig. 7d). Fig. 7c shows the variation of $\dfrac{C_1}{R_1}$ from the phasor diagrams (curve A) and from Eq. (21) (curve B) for different values of frequency ω (cf. Table 3).

www.czasopisma.pan.pl PAN www.journals.pan.pl

POLSKA AKADEMIA NAUK

INVESTIGATION OF LIMIT CYCLES AND SIGNAL STABILIZATION
OF TWO DIMENSIONAL SYSTEMS WITH MEMORY TYPE NONLINEAR ELEMENTS 299

Table 3: Values of different quantities for Example 2: for backlash: $D_1 = 2.16$, $D_2 = 1.26$, $b_1 = b_2 = 1.0$; $X_{m1} = 2.3$, $X_{m2} = 1.4$

ω (rad/sec)	θ_{L_1} (in degrees)	θ_{L_2} (in degrees)	$\dfrac{C_1}{R_1}$ from plot OD_1, OD_2	$\dfrac{C_1}{R_1}$ from Eq. (21)
0.600	-166.3940	-121.8119	0.8554, 4.2227	9.8200
0.625	-168.4773	-122.1618	0.8616, 4.9186	9.6127
0.650	-170.5142	-122.5110	0.8720, 5.8676	9.4065
0.675	-172.5052	-122.8596	0.8869, 7.2609	9.2017
0.700	-174.4505	-123.2074	0.9064, 9.5447	8.9988
0.6961	-174.1500	-123.1532	0.9031, 9.0955	9.0303
0.6955	-174.1037	-123.1448	0.9025, **9.0302**	**9.0351**

The point of the intersection of curve (A) and curve (B) provides the value of limit cycle frequency $\omega = 0.6955$ rad/sec. Other values of interest are determined from the Fig. 7d as:

$$\frac{C_1}{R_1} = 9.0302; \quad \frac{X_1}{R_1} = 8.6090;$$
$$\frac{C_2}{R_1} = 1.0; \quad \frac{X_2}{R_1} = 9.5381.$$

Thus,

$$X_1 = X_{m1}N_1G_1\frac{BD}{OD} = 4.4220,$$
$$X_2 = X_{m2}N_2G_2\frac{AD}{OD} = 4.8965,$$
$$C_1 = 4.6384,$$
$$C_2 = 0.5136,$$

where, X_{m1} and X_{m2} are amplitudes of sinusoids for subsystems S_1 and S_2 respectively.

Following the similar steps as has been illustrated in section 2.1.2, the digital simulation for the example 2 is done.

The results of the digital simulation are shown in Fig. 8 and compared in Table 4 with the results obtained from the graphical method.
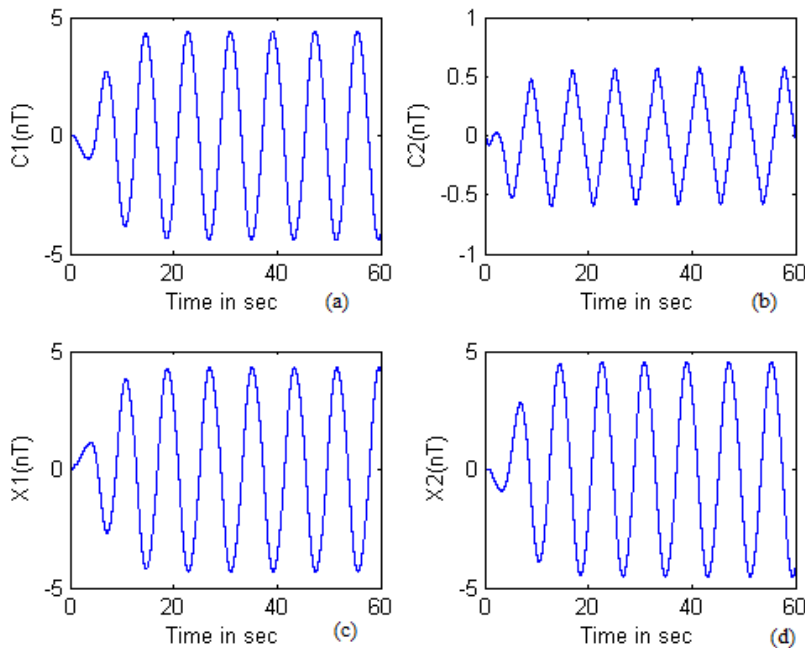
Figure 8: Results of Example 2 for C_1, C_2, X_1, and X_2 obtained from digital simulation

Table 4: Comparison of results of Example 2

Methods of computation	ω (rad/sec)	X_1	X_2	C_1	C_2
Graphical	0.6955	4.42	4.89	4.63	0.51
Digital simulation	0.76	4.30	4.51	4.39	0.57

C. Signal stabilization

The system shown in Fig. 1 exhibits a limit cycle in the autonomous state. The possibility of quenching the limit cycle by injecting suitable high frequency signals [12, 17, 20–22, 24] at the two inputs is shown below. When the amplitude B_1 of sinusoidal input $B_1 \sin \omega_f t$ is gradually increased keeping the amplitude of forcing signal $B_2 \sin \omega_f t$ fixed, the system would continue to exhibit a limit cycle. The variables at various points in the system would be composed of signals of the input frequency (ω_f), the frequency of self oscillations (ω_s) and the combination of frequencies, $k_1 \omega_f \pm k_2 \omega_s$ where k_1, k_2, assume various integers values.

However as the magnitude B_1 is gradually increased the frequency of self oscillations, ω_s, would also gradually change. For a certain magnitude of the

www.czasopisma.pan.pl   PAN   www.journals.pan.pl

POLSKA AKADEMIA NAUK

INVESTIGATION OF LIMIT CYCLES AND SIGNAL STABILIZATION
OF TWO DIMENSIONAL SYSTEMS WITH MEMORY TYPE NONLINEAR ELEMENTS   301

input, synchronization would occur i.e. the self-oscillations would be quenched and the system would exhibit forced oscillations at frequency ω_f. If subsequently the amplitude B_1 is reduced a point may be reached at which the self oscillations would reappear (i.e. desynchronization would take place). It may be noted that for each given B_2, the amplitude B_1 for synchronization in general, be larger than that for desynchronization.

C.1.   Rectangular hysteresis

C.1.1.   Complex oscillation

Considering the system of Fig. 1, a high frequency signal $B\sin\omega_f t$ may be injected at u_1 keeping u_2 unexcited as shown in Fig. 9a.
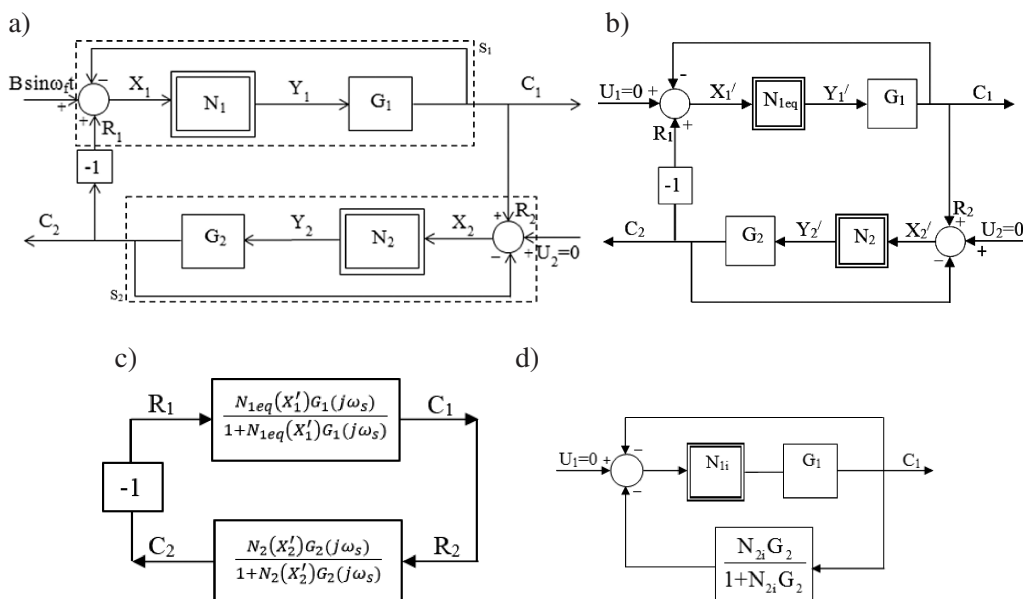

Figure 9: a) Equivalent system for forced oscillations, b) equivalent system for analysing complex oscillations, c) inearized equivalent of the system, d) equivalent linearization for incremental signals for the system of Fig. 6a

If the amplitude (B) of the high frequency signal is gradually increased, the system would exhibit complex oscillations [28, 31]. In the process for a certain value of amplitude B, synchronization would occur where the self-oscillation would vanish and the system would exhibit forced oscillations at the frequency ω_f [20]. On the reverse operation, if the amplitude B is gradually reduced, at certain value of B the self-oscillations i.e. the limit cycle would reappear and the system would exhibit complex oscillations, which is termed as desynchroniza-tion phenomenon [12, 17, 21, 22, 24, 31].

The process of complex oscillations with synchronization and desynchronization has been analysed through subsequent development of Figs 9b, c and d, illustrated through example 3 and the results of which are shown in Fig. 10a, b, c and d.
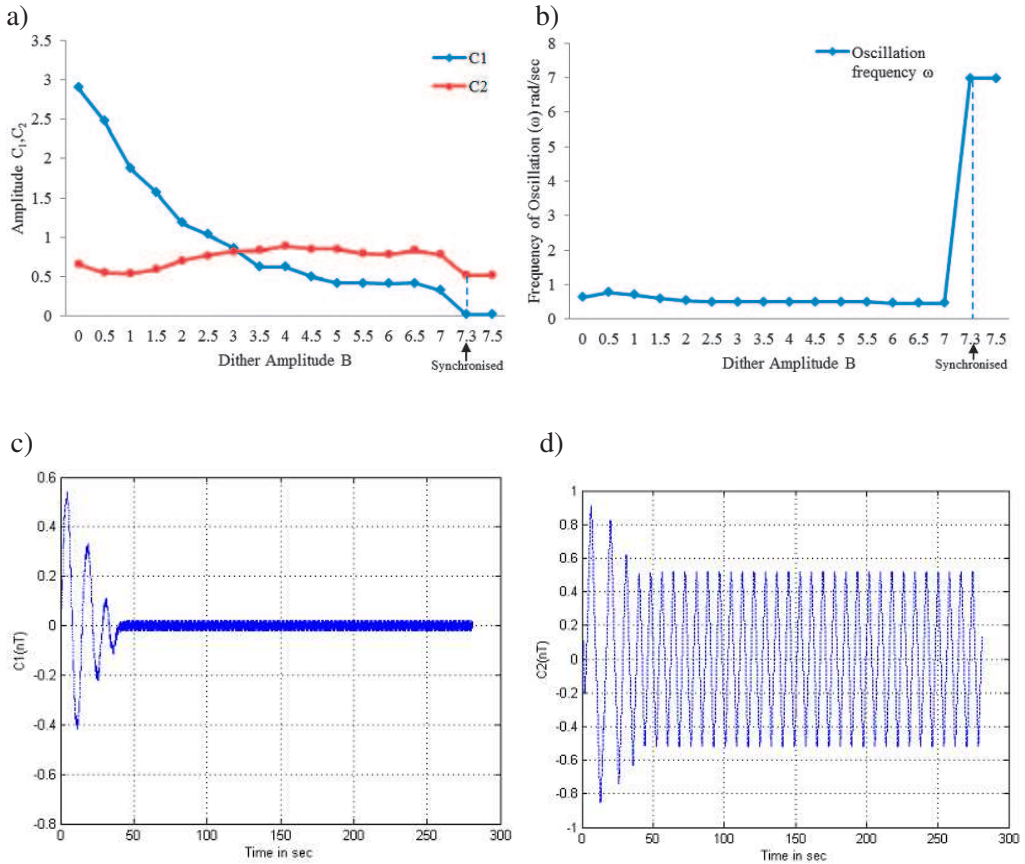
a)

b)

c)

d)

Figure 10: Results of the system in Example 3 using digital simulation method: a) variation of C_1, C_2 with Dither amplitude B, b) variation of ω with Dither amplitude B, c) synchronization of C_1 with forcing frequency, d) synchronization of C_2 with forcing frequency

Example 3

Consider the system of Fig. 1 with $U_1 = B\sin\omega_f t$, the equivalent DIDF [22] is being used for prediction of forced oscillations. $G_1(s)$, $G_2(s)$, N_1, N_2 remain the same as in the example1. The equivalent DIDF [27] for Rectangular Hysteresis in the subsystem S_1 is given by

$$N_A(B,A) = \frac{M_1}{\pi A}\left[\sin^{-1}\left(\frac{h+A}{B}\right) - \sin^{-1}\left(\frac{h-A}{B}\right)\right], \qquad (22)$$

www.czasopisma.pan.pl   PAN   www.journals.pan.pl
POLSKA AKADEMIA NAUK

INVESTIGATION OF LIMIT CYCLES AND SIGNAL STABILIZATION
OF TWO DIMENSIONAL SYSTEMS WITH MEMORY TYPE NONLINEAR ELEMENTS   303

where input to the nonlinear element N_1 is $X_1 \sin \omega_s t + B \sin \omega_f t$; $\dfrac{\omega_f}{\omega_s} \to \infty$ (high value). X_1 and B are amplitudes of sinusoids: X_1 is the amplitude of limit cycle, B is the amplitude of high frequency signal and A = Average value of X_1 i.e. $\dfrac{2X_1}{\pi}$.

During the process of signal stabilization, keeping frequency ω_f at 7 rad/sec (at least 10 times of ω_s), the amplitude B of forcing signal is gradually increased till quenching of self-oscillation. The corresponding value of B is taken as synchronization amplitude. Similarly, in the reverse operation, keeping ω_f constant, gradually the amplitude B is reduced and the value of B for desynchronization is noted. The results of forced oscillations are shown in Table 5 and also presented in Fig. 10.

Table 5: Forced oscillations of Example 3 with $M_1 = 1.0$, $M_2 = 1.126$, $\omega_f = 7$ rad/sec

B	C_1	C_2	ω (rad/sec)	Remarks
0	2.901	0.6598	0.6347	
1.0	1.881	0.5413	0.7757	
2.0	1.188	0.7071	0.5817	
3.0	0.8639	0.8207	0.5031	
4.0	0.6246	0.8888	0.4833	
5.0	0.4178	0.8507	0.4833	
6.0	0.4155	0.7861	0.4833	
7.0	0.3293	0.7858	0.4833	
7.3	0.0192	0.5127	6.9813	**Synchronization**
8.0	0.0192	0.5176	6.9813	

Based on the assumptions [23–25], the input to the nonlinear element N_1 is composed of sinusoidal signals of frequencies ω_s and ω_f while the input to the nonlinear element N_2 is composed only of a sinusoidal signal of frequency ω_s. The equivalent system for Fig. 10a under complex oscillation is shown in Fig. 10b and the linearized equivalent is shown in Fig. 10c, where N_1eq is the Dual Input Describing function (DIDF) [1, 6, 27] and N_2 is the single sinusoidal input Describing function (DF) for the self-oscillating signal of frequency ω_s only.

Considering the steps outlined in [23–25], the conditions for the existence of complex oscillations with memory type nonlinearity can be written as:

i. The Phase angle condition

$$\theta_{c_1} + \theta_{c_2} = 180^\circ, \tag{23a}$$

where $\theta_C =$ loop angles of subsystems which include the angles of N_1 and N_2.

$$\theta_{C1} = \mathrm{Arg}\left(\frac{G_1(j\omega)N_1(X_1,\omega)}{1+G_1(j\omega)N_1(X_1,\omega)}\right),$$

$$\theta_{C2} = \mathrm{Arg}\left(\frac{G_2(j\omega)N_2(X_2,\omega)}{1+G_2(j\omega)N_2(X_2,\omega)}\right),$$

$$\theta_{L_1} = \angle G_1(j\omega) + \angle - \sin^{-1}\frac{H}{2X_1'},$$

$$\theta_{L_2} = \angle G_2(j\omega) + \angle - \sin^{-1}\frac{H}{2X_2'}.$$

ii. The gain condition

$$\frac{C_1}{R_1} \times \frac{C_2}{R_2} = 1. \tag{23b}$$

iii. The amplitude ratio condition

$$\frac{X_1'}{X_2'} = \frac{|1+N_2G_2(j\omega)|}{|N_1G_1(j\omega)|}. \tag{23c}$$

Eq. (23) constitutes three relations with three unknowns: ω, X_1, and X_2, which can be solved by analytical method/graphical method/digital simulation/ use of MATLAB/SIMULINK.

C.1.2. Digital simulation

The steps depicted in section 2.1.2 for example1 are followed for Example 3 here. The Results of Forced oscillations using digital simulation for Example 3 showing the synchronization of the system with the forcing signal are given in Table 5. The variations of C_1 and C_2 and ω with dither amplitude B obtained from digital simulation are shown in Fig. 10a and b, respectively.

During the process of signal stabilization, the values of C_1 and C_2 synchronised with forcing frequency are shown in Fig. 10c and d, respectively.

C.1.3. Desynchronization

In the process of forced oscillation for a reasonably large B, the self-oscillations would be quenched and the system would synchronise to forced oscillations at frequency ω_f.

Because of low pass characteristics of the system, the output C_1 and C_2 are assumed to be negligibly small. Hence, the inputs to the nonlinear elements N_1 and N_2 can be approximated $B\sin\omega_f t$ and a vanishingly small signal.

www.czasopisma.pan.pl   PAN   www.journals.pan.pl
POLSKA AKADEMIA NAUK

INVESTIGATION OF LIMIT CYCLES AND SIGNAL STABILIZATION
OF TWO DIMENSIONAL SYSTEMS WITH MEMORY TYPE NONLINEAR ELEMENTS   305

If B is gradually reduced the self-oscillations would reappear [22, 28, 31] at a point at which the forced oscillations become unstable and this instability can be predicted by employing Incremental input Describing function (IDF) [31].

The limiting value of B at which the self-oscillations reappear can be determined by replacing the nonlinear elements N_1 and N_2 by their IDFs i.e. N_{1i} and N_{2i} for vanishingly small signals superimposed on the finite amplitude signal of frequency ω_f at their respective inputs.

The linearized equivalent for incremental input signals of the systems of Fig. 9(b) is shown in Fig. 9(d). The condition for self-oscillations for just reappearance is obtained as:

$$\left[1 + N_{1i}G_1(j\omega)\left[1 + \left(\frac{N_{2i}G_2(j\omega)}{1 + N_{2i}G_2(j\omega)}\right)\right]\right] = 0. \tag{24}$$

Eq. (19) implies that N_{1i} is the slope at the origin of the modified characteristic of N_1 for an input $B\sin\omega_f t$, while N_{2i} is the slope at the origin of the characteristic of N_2 [22, 24, 28, 31].

Example 4

Example 3 is revisited in the line of Fig. 9d for forced oscillation. For a vanishingly small signal X_{2s}, the N_{2i} for the rectangular hysteresis would tend to be infinity.

Hence,

$$\frac{N_{2i}G_2(j\omega)}{1 + N_{2i}G_2(j\omega)} \simeq 1.$$

Hence Eq. (24) yields

$$1 + 2N_{1i}G_1(j\omega) = 0, \tag{25}$$

where

$$N_{1i} = \frac{2M_1}{\pi B}\frac{1}{\sqrt{1 - \left(\frac{H}{2B}\right)^2}} = 0.5. \tag{26}$$

Substituting $G_1(j\omega)$ and separating the real and imaginary parts of Eq. (24) we get,

$$2N_{1i} - \omega^2 = 0 \quad \text{and} \quad 1 - \omega^2 = 0 \quad \text{or} \quad 2N_{1i} - 1 = 0 \quad \text{or} \quad N_{1i} = 0.5.$$

From Eq. (26),

$$\frac{2M_1}{\pi B\sqrt{1 - \left(\frac{H}{2B}\right)^2}} = 0.5, \qquad \text{where} \quad M_1 = 1, \quad H = 1.$$

Hence,

$$\frac{2}{\pi B\sqrt{1-\left(\frac{1}{2B}\right)^2}} = 0.5, \qquad \frac{2}{0.5} = \pi B\sqrt{1-\left(\frac{1}{2B}\right)^2}$$

or

$$1-\left(\frac{1}{2B}\right)^2 = \left(\frac{4}{\pi B}\right)^2 \quad \text{or} \quad B^2 - \left(\frac{4}{\pi}\right)^2 = \frac{1}{4}$$

or

$$B = \sqrt{\frac{1}{4}+\left(\frac{4}{\pi}\right)^2} = \sqrt{1.871} = 1.367 = B_d$$

(Desynchronization value of B).

Results of forced oscillations using digital simulation for Example 4 showing the desynchronization of the system are given in Table 6. Results of digital simulation shows desynchronization at $B_d = 1.8$.

Table 6: Results of forced oscillations for Example 4 with $M_1 = 1.0$, $M_2 = 1.126$, $\omega_f = 7$ rad/sec

B	C_1	C_2	ω	Remarks
8.0	0.0192	0.5176	6.9813	
7.0	0.0192	0.5176	6.9813	
6.0	0.0192	0.5176	6.9813	
5.0	0.4178	0.7970	0.5027	
4.0	0.6246	0.8888	0.4987	
3.0	0.7181	0.8313	0.4987	
2.0	1.151	0.705	0.5872	
1.9	1.304	0.6892	0.6160	
1.8	1.450	0.6361	0.6545	**Desynchronization**
1.7	1.511	0.6103	0.6604	
1.6	1.564	0.5846	0.6981	
1.5	1.678	0.5808	0.7060	
1.0	1.885	0.5413	0.7662	

www.czasopisma.pan.pl   PAN   www.journals.pan.pl
POLSKA AKADEMIA NAUK

INVESTIGATION OF LIMIT CYCLES AND SIGNAL STABILIZATION
OF TWO DIMENSIONAL SYSTEMS WITH MEMORY TYPE NONLINEAR ELEMENTS   307

C.2. Backlash nonlinearity

C.2.1. Forced oscillation

When the system of Fig. 1 exhibits self oscillations while being subjected to the high frequency inputs $B_1 \sin \omega_f t$ and $B_2 \sin \omega_f t$ at u_1 and u_2 respectively the behaviour of the system can be analysed by replacing the nonlinear elements N_1 and N_2 by their modified characteristics [28, 31] determined by the components of the frequency ω_f at their inputs, thus leading to the Fig. 9d as a linear equivalent. The condition for existence of forced/complex oscillations under such situation is derived as [21].

$$G_1(j\omega)N_{1eq} + G_2(j\omega)N_{2eq} + 2G_1(j\omega)G_2(j\omega)N_{1eq}N_{2eq} = -1 \qquad (27)$$

and

$$\frac{X_1'}{X_2'} = \left| \frac{N_{1eq}G_1(j\omega)}{1 + N_{2eq}G_2(j\omega)} \right|, \qquad (28)$$

where N_{1eq} and N_{2eq} are the DFs for the modified characteristics (DIDFs of the original nonlinear elements) forming the respective nonlinear elements of the system of Fig. 9d and X_1', X_2' are the inputs to the respective non linear elements. In the process of signal stabilization two important phenomena [28, 31] like synchronization and desynchronization are observed. The synchronization is determined with the use of Dual Input Describing Function (DIDF) which is very complex for backlash nonlinearities [27]. The desynchronization is determined with the use of Incremental Describing Function (IDF) which is simple to determine.

C.2.2. Determination of stability boundary

Let the system of Fig. 9a be subjected to high frequency inputs, $B_1 \sin \omega_f t$ and $B_2 \sin \omega_f t$ at U_1 and U_2 respectively. Consider the situation for reasonably large signal, when the self oscillations have been quenched and consequently the system is exhibiting a harmonic oscillation at the forcing frequency (dealt in subsequent section). Since the frequency of the forcing signal is high, the magnitude of outputs C_1 and C_2 can be assumed to be negligibly small.

It has been seen that when the forcing signal is gradually reduced, the self oscillation would reappear at a point at which the forced oscillations becomes unstable and that this instability can be predicted by employing incremental input describing functions (IDF) [6, 31].

Hence, the limiting values of the forcing signals at which the self oscillations reappear can be obtained by analysing the stability boundary of the equivalent linear system obtained by replacing the nonlinear elements N_1 and N_2 by their respective IDFs, N_{1i} and N_{2i} (these are gains for vanishingly small signals of an incommensurate frequency superimposed on the finite amplitudes of the forcing

signals of frequency ω_f at their respective inputs). The equivalent linear system for incremental signals is shown in Fig. 9d and its stability boundaries can therefore be obtained by applying Routh-Hurwitz Criterion.

The following specific example is intended to illustrate the procedure for the analysis of this phenomenon and outline the distinct stability boundary (in the K_1-K_2 plane) of the system obtained for occurrence of limit cycles and quenching of such oscillations through digital simulations.

Example 5

Consider the system of Fig. 9a, where $G_1(s) = \dfrac{2}{s(s+1)^2}$; $G_2(s) = \dfrac{1}{s(s+4)}$ and the two nonlinear elements have backlash type characteristics shown in Fig. 6 with $b_1 = b_2 = 1.0$, slopes $K_1 = 1.2$, $K_2 = 1.4$ and $D_1 = 2.16$ and $D_2 = 1.26$ respectively. The occurrence of limit cycles is predicted leading to the stability boundary of the linear equivalent system in sequel. The system is forced with high frequency signals $B_1 \sin \omega_f t$ and $B_2 \sin \omega_f t$ at u_1 and u_2 respectively. Let the system be oscillating (after synchronization) at frequency ω_f and can be evaluated [21, 31] from the stability boundary in the K_1/K_2 plane of the linear equivalent for incremental signals of the system shown in Fig. 9d, wherein the nonlinear elements have been replaced by their incommensurate IDF's. The equivalent characteristic equation for this system is obtained as:

$$s^5 + 6s^4 + (9 + N_{2i})s^3 + (4 + 2N_{1i} + 2N_{2i})s^2 + (8N_{1i} + N_{2i})s + 4N_{1i}.N_{2i} = 0, \quad (29)$$

N_{1i} (For Back lash nonlinearity) $= K_1$, the slope of N_1 and N_{2i} (for Back lash non linearity) $= K_2$, the slop of N_2. The IDF for backlash nonlinearity has been derived in Appendix A2 [1, 6, 31]. Replacing N_{1i} and N_{2i} by K_1 and K_2 respectively in Eq. (29) and the equivalent characteristics equation of the systems of Example 5 becomes:

$$s^5 + 6s^4 + s^3(9 + K_2) + s^2(4 + 2K_1 + 2K_2) + s(8K_1 + K_2) + 4K_1K_2 = 0. \quad (30)$$

Employing the Routh-Hurwitz criterion from Eq. (30), the stability boundary of the system in terms of K_1 and K_2 is derived in Appendix A3. Table 7 is prepared for different values of K_2 with the computed values of K_1 from Eqs. (A3-1), (A3-2) and (A3-4) respectively. Utilizing the data from Table 7, Fig. 11 is drawn showing the stability boundary in K_1/K_2 plane. The boundary confirms no occurrence of limit cycle within it.

Employing the Routh-Hurwitz criterion from Eq. (30), the stability boundary of the system in terms of K_1 and K_2 is derived in Appendix A3. Table 7 is prepared for different values of K_2 with the computed values of K_1 from Eqs. (A3-1), (A3-2) and (A3-4) respectively. Utilizing the data from Table 7, Fig. 11 is drawn showing the stability boundary in K_1/K_2 plane. The boundary confirms no occurrence of limit cycle within it.

www.czasopisma.pan.pl   PAN   www.journals.pan.pl
POLSKA AKADEMIA NAUK

INVESTIGATION OF LIMIT CYCLES AND SIGNAL STABILIZATION
OF TWO DIMENSIONAL SYSTEMS WITH MEMORY TYPE NONLINEAR ELEMENTS   309

Table 7: Stability Boundary of system for Example 5

K_2	K_1 (Degree 1) Eq. (A3-1) for stability $K_1 >$	K_1 (Degree 2) Eq. (A3-2) for stability $K_1 >$	K_1 (Degree 3) Eq. (A3-5) r for stability $K_1 <$
0	25	1.0	1.0
1	27	1.6495	0.50976
2	29	2.6060	0.3315
3	31	4	0.30643
4	33	6	0.30765
5	35	8.7797	0.31552
6	37	12.4452	0.32515
7	39	16.9706	0.33492
8	41	22.1250	0.34425
9	43	28	0.35293
10	45	34.1696	0.36092
11	47	40.6083	0.36824
12	49	47.2363	0.37493
13	51	54	0.38104
14	53	60.8628	0.38664
15	55	67.7995	0.39177
16	57	74.7926	0.39649
17	59	81.8295	0.40084
18	61	88.9009	0.40486
19	63	96	0.40858
20	65	103.1216	0.41203

C.2.3. Synchronization

When the system is exhibiting a limit cycling in autonomous state, one of the way to quench the limit cycle by enforcing high frequency dither signal [17, 21, 22, 28, 31] at the relevant point in the loop as shown in Fig. 9a. The method of digital simulation as outlined in section 2.1.2 is followed for determination of a synchronization boundary and has been illustrated through the example.

Example 5 is revisited: Using the method of digital simulation for a fixed value of B_2, B_1 is gradually increased; the oscillations are quenched, at a particular value of B_1 the system is synchronized to forcing frequency ω_f. The results
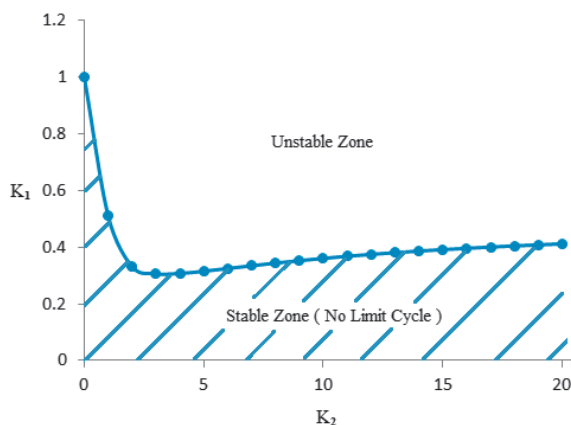
Figure 11: * Stability boundary for the system of Example 5

* For clarity of the Fig. 11 the boundary derived from degree 2 and 1 of s (in Routh-Hurwitz Criterion) are not shown. The boundary derived with the most stringent conditions of degree 3 of s (Routh-Hurwitz Criterion) only is shown.

of synchronization values of B_1 for different fixed values of B_2 are shown in Table 8 and plotted in Fig. 12a. The synchronization boundary in $B_2 - B_1$ plane is shown in Fig. 12b.

Table 8: Forced oscillations of Example 5 with $\omega_f = 7$ rad/sec

B_2	B_1	C_1	C_2	ω	Remarks
	0.5	4.572	0.5745	0.7570	
	1.0	3.781	0.5221	0.8055	
	2.0	3.114	0.5065	0.8267	
	3.0	1.798	0.5537	0.7222	
	4.0	1.240	0.6261	0.5764	
	5.0	1.024	0.6469	0.5027	
0	6.0	0.8797	0.6805	0.4654	
	7.0	0.8144	0.6884	0.4394	
	8.0	0.7033	0.6858	0.4363	
	9.0	0.6139	0.6464	0.4217	
	9.5	0.514	0.6022	0.4363	
	9.6	0.5128	0.6144	0.4363	
	9.7	**0.0394**	**0.0155**	**6.9813**	**Synchronized**
	9.8	0.0400	0.0159	6.9814	

www.czasopisma.pan.pl PAN www.journals.pan.pl
POLSKA AKADEMIA NAUK

INVESTIGATION OF LIMIT CYCLES AND SIGNAL STABILIZATION
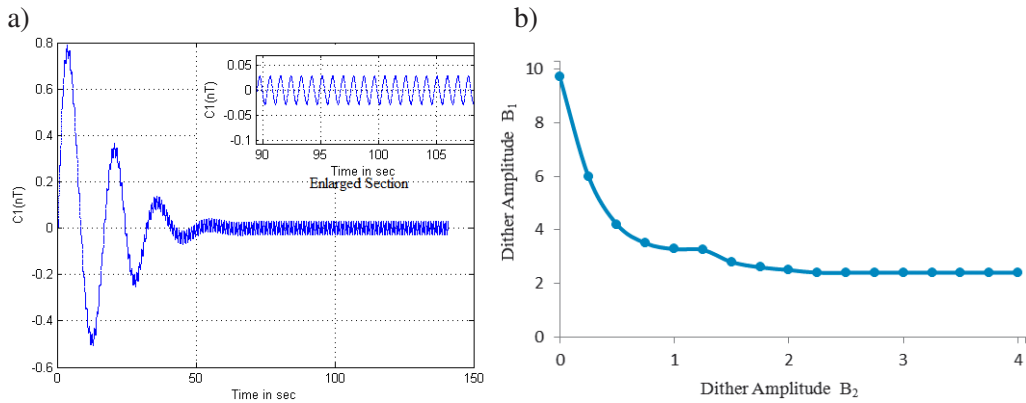OF TWO DIMENSIONAL SYSTEMS WITH MEMORY TYPE NONLINEAR ELEMENTS   311

a)

b)

Figure 12: a) Synchronization of C_1 with forcing frequency, b) Quenching of oscillations by signal stabilization

D.   General 2×2 nonlinear systems

D.1.   Graphical method

Consider the general 2×2 nonlinear system [25, 26] as shown in Fig. 13. From the block diagram of Fig. 13 we get,

$$R_1 = C_1 + E_1, \quad C_2 = R_2, \quad R_2 = C_2 + X_2, \quad R_1 = -C_3,$$

$$C_2 = -\frac{R_1}{G_3}.$$

Accordingly, the normalised phasor diagram for a sustained limit cycle of the system of Fig. 13 is shown in Fig. 14a. The phasor diagram is normalised with respect to amplitude R_1.
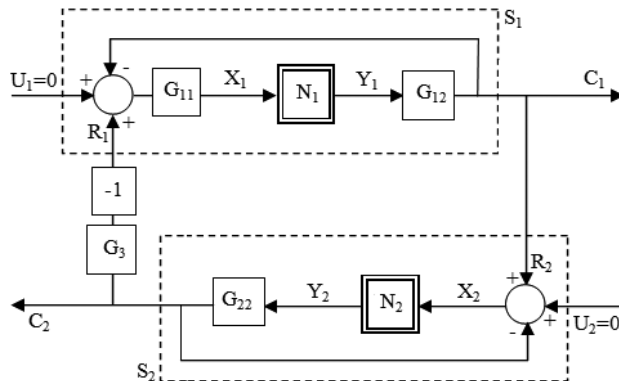
Figure 13: General 2×2 Nonlinear Systems

a)

b)

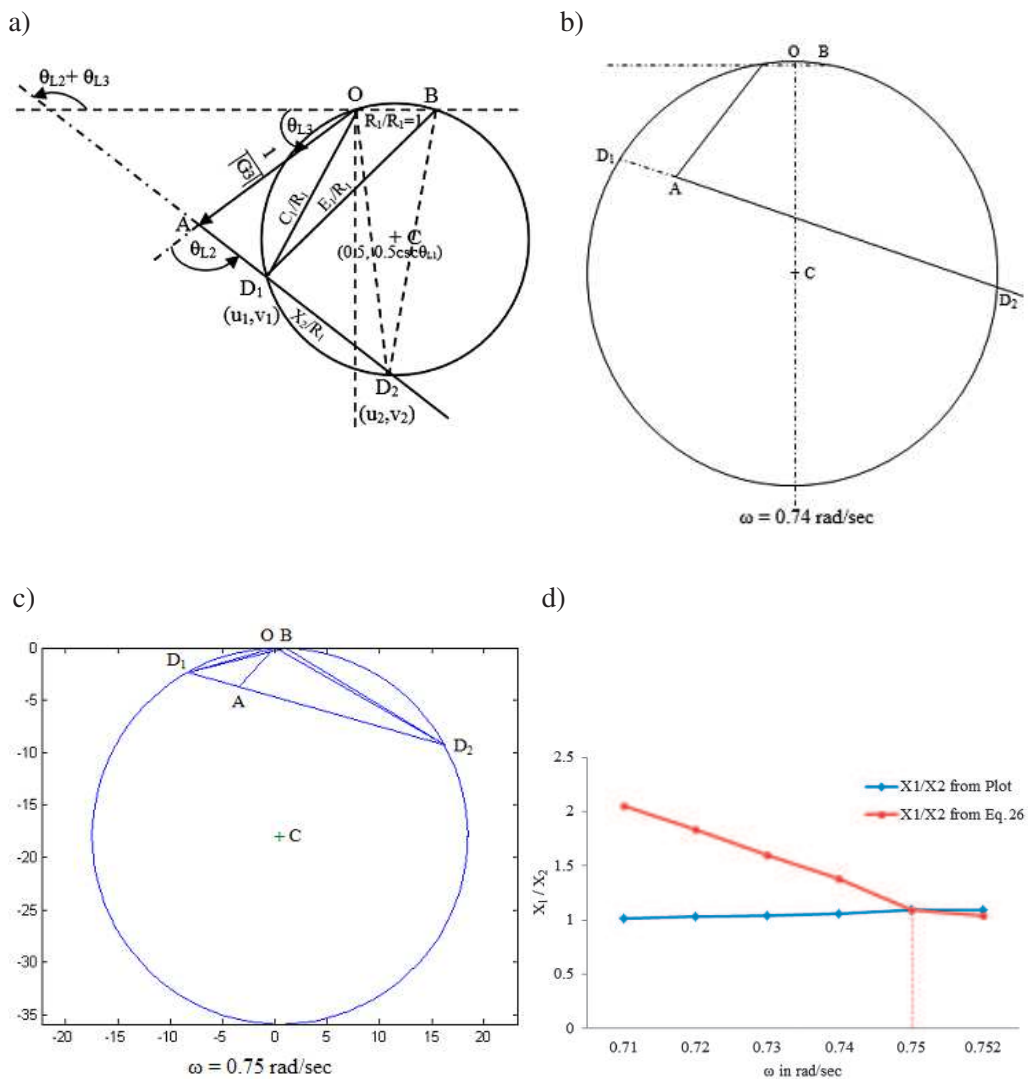$\omega = 0.74$ rad/sec

c)

$\omega = 0.75$ rad/sec

d)

Figure 14: Graphical representation of the system in Example 6: a) normalised phasor diagram for most general 2×2 nonlinear system of Fig. 13, b) normalised phasor diagram for the system in Example 6 with $\omega = 0.74$ rad/sec, c) normalised phasor diagram with $\omega = 0.75$ rad/sec for final solution, d) final solution of the system in Example 6 corresponding to Table 9

Centre of the circle is at $\left(\dfrac{1}{2}, \dfrac{-1}{2\tan\theta_{L1}} \right)$ with radius, $r = \dfrac{1}{2}\sin\theta_{L1}$.

Coordinate of point A $\left(\dfrac{1}{G_3}\cos(\pi + \theta_{L3}), \dfrac{1}{G_3}\sin(\pi + \theta_{L3}) \right)$.

www.czasopisma.pan.pl PAN www.journals.pan.pl
POLSKA AKADEMIA NAUK

INVESTIGATION OF LIMIT CYCLES AND SIGNAL STABILIZATION
OF TWO DIMENSIONAL SYSTEMS WITH MEMORY TYPE NONLINEAR ELEMENTS   313

Coordinates of D_i are u_i and v_i, where $i = 1, 2$.
Let

$$\alpha = \frac{1}{G_3}\{\sin(\pi + \theta_{L3})\cot(\theta_{L2} + \theta_{L3}) - \cos(\pi + \theta_{L3})\},$$

$$\lambda = 2\cot(\theta_{L2} + \theta_{L3})\left(\alpha + \frac{1}{2}\right) + \cot\theta_{L1},$$

$$v_i = \frac{\lambda \pm \sqrt{\lambda^2 - 4\cos\mathrm{ec}^2(\theta_{L2} + \theta_{L3})\alpha(\alpha + 1)}}{2\cos\mathrm{ec}^2(\theta_{L2} + \theta_{L3})},$$

$$u_i = v_i\cot(\theta_{L2} + \theta_{L3}) - \alpha,$$

where,

$$\theta_{L1} = \arg\left(G_{11}(j\omega)\right) + \arg\left(G_{12}(j\omega)\right) + \arg(N_1(X, \omega)),$$
$$\theta_{L2} = \arg\left(G_{22}(j\omega)\right) + \arg(N_2(X, \omega)),$$
$$\theta_{L3} = \arg(G_3(j\omega)),$$
$$OB = \frac{R_1}{R_1} = 1.0,$$
$$OA = \frac{C_2}{R_1} = \frac{1}{|G_3|},$$
$$OD_i = \frac{C_1}{R_1}, \quad BD_i = \frac{E_1}{R_1}, \quad AD_i = \frac{X_2}{R_1} \quad (i = 1, 2).$$

The phasor diagram for a given ω yields

$$\frac{OD_i}{BD_i} = \frac{C_1/R_1}{E_1/R_1} = (N_1)_i G_{11}G_{12},$$
$$\frac{OA}{AD_i} = \frac{C_2/R_1}{X_2/R_1} = (N_2)_i G_{22}$$

or

$$\frac{1}{AD_i G_3} = (N_2)_i G_{22},$$

where $(N_1)_i$ and $(N_2)_i$ are the two DFs corresponding to the points D_i with $i = 1$ and 2 respectively. This finally gives the following results:

$$(N_1)_i = \frac{OD_i}{BD_i G_{11}G_{12}}, \tag{31}$$

$$(N_2)_i = \frac{1}{AD_i G_{22}G_3} \tag{32}$$

and

$$\frac{X_1}{X_2} = \frac{BD_i G_{11}}{AD_i} \tag{33}$$

(This can be determined from the phasor diagram).

Eq. (24) can also be written as

$$\frac{X_1}{X_2} = \frac{BD_i |G_{11}|}{AD_i} = |G_{11}| \sqrt{\frac{(u-1)^2 + v^2}{\left(u - \frac{1}{|G_3|}\cos(\gamma)\right)^2 + \left(v - \frac{1}{|G_3|}\sin(\gamma)\right)^2}} \tag{34}$$

(This can also be computed analytically) where $\gamma = \pi + \theta_{L3}$.

Considering the magnitude ratios only from the respective DFs,

$$\frac{X_1}{X_2} = \frac{M_1}{M_2} \times \frac{(N_2)_i}{(N_1)_i} = \frac{1}{1.126} \times \frac{OD_i AD_i G_{22} G_3}{BD_i G_{11} G_{12}}, \tag{35}$$

where $(N_1)_i$ and $(N_2)_i$ are determined from phasor diagram in conjunction with Eqs. (31) and (32).

Equations (31)–(35), with the aid of phasor diagram Fig. 14b and c, yield numerical values for N_1, N_2 and $\frac{X_1}{X_2}$ for a given value of ω. The comparison of the ratio $\frac{X_1}{X_2}$ obtained by two independent ways is best done by plotting $\frac{X_1}{X_2}$ against ω. The point of intersection of the two curves ensures their equality and thus yields the frequency of limit cycle. Once ω is determined, the amplitudes of other variables of interest are calculated directly from the expressions developed.

This procedure is repeated for several values of ω. The frequency of limit cycle is found to be the frequency for which $\frac{X_1}{X_2}$, for a particular value of i (1 or 2), determined by both routes are the same. The amplitudes of several other variables can subsequently be calculated. This procedure is illustrated through the Example 6.

Example 6

Consider the system of Fig. 13

$$G_{11}(s) = s+1, \qquad G_{12}(s) = \frac{2}{s(s+1)^3},$$

$$G_{22}(s) = \frac{1}{s(s+4)}, \qquad G_3(s) = \frac{1}{(s+1)(s+4)}.$$

www.czasopisma.pan.pl   PAN   www.journals.pan.pl

POLSKA AKADEMIA NAUK

INVESTIGATION OF LIMIT CYCLES AND SIGNAL STABILIZATION
OF TWO DIMENSIONAL SYSTEMS WITH MEMORY TYPE NONLINEAR ELEMENTS   315

N_1, N_2 represent the nonlinearities of subsystem S_1 and S_2 having rectangular hysteresis characteristics with $M_1 = 1.0$ and $M_2 = 1.126$ respectively.

$$\theta_{L1} = \tan^{-1}\omega - \sin^{-1}\frac{H}{2X_1} - \frac{\pi}{2} - 3\tan^{-1}\omega,$$

$$\theta_{L2} = -\frac{\pi}{2} - \tan^{-1}\frac{\omega}{4} - \sin^{-1}\frac{H}{2X_2},$$

$$\theta_{L3} = -\tan^{-1}\omega - \tan^{-1}\frac{\omega}{4}.$$

For different values of ω, the relevant data used for drawing normalised phasor diagrams to scale are shown in Table 9 and normalised phasor diagrams are drawn using computer graphics as shown in Fig. 14b and 14c. A tentative solution for matching $\dfrac{X_1}{X_2}$ is shown in Table 9.

Table 9: Values of different quantities for Example 6

ω	θ_{L_1}	θ_{L_2}	θ_{L_3}	$\dfrac{X_1}{X_2}$ (Plot)	$\dfrac{X_1}{X_2}$ (Eq. (26))
0.71	-173.64	-111.37	-45.43	18.08, 1.0969	69.4784, 2.6215
0.72	-174.40	-111.51	-45.95	8.5556, 1.0944	30.4845, 2.3881
0.73	-175.15	-111.65	-46.47	5.8363, 1.0796	19.5513, 2.1220
0.74	-175.90	-111.78	-46.98	4.4018, 1.0677	13.6981, 1.8985
0.75	-176.63	-111.92	-47.48	3.4906, 1.0908	10.1127, 1.6633
0.76	-177.36	-112.06	-47.99	2.9067, 1.1066	7.5908, 1.4298
0.77	-178.09	-112.20	-48.49	2.4685, 1.1269	5.7058, 1.1641
0.771	-178.18	-112.22	-48.55	2.4981, **1.1267**	5.6682, **1.1203**
0.775	-178.44	-112.27	-48.74	2.2391, 1.1345	4.5870, 1.0253

The above process is reiterated by taking the values $X_1 = 1.975$, $X_2 = 1.768$ and shown in Table 6, which has been finally obtained with the help of Fig. 9d.

The limit cycles exhibited at $\omega = 0.75$ rad/sec where $X_1 = 2.074$, $X_2 = 1.891$, $C_1 = 1.737$ and $C_2 = 0.469$.

Table 10: Final solution of the system in Example 6, limit cycles exhibited at $\omega = 0.75$ rad/sec where $X_1 = 2.074$, $X_2 = 1.891$, $C_1 = 1.737$ and $C_2 = 0.469$

ω	θ_{L_1}	θ_{L_2}	θ_{L_3}	$\dfrac{X_1}{X_2}$ (Plot)	$\dfrac{X_1}{X_2}$ (Eq. (26))
0.71	-175.414	-116.493	-45.440	5.5188, 1.0163	18.3946, 2.0532
0.72	-176.173	-116.632	-45.958	4.1557, 1.0285	12.9171, 1.8326
0.73	-176.924	-116.770	-46.472	3.3087, 1.0407	9.3236, 1.6016
0.74	-177.668	-116.909	-46.983	2.7788, 1.0597	6.8997, 1.3784
0.75	-178.405	-117.047	-47.489	2.3762, **1.0914**	5.1447, **1.0964**
0.752	-178.550	-117.075	-47.590	2.2957, 1.0940	4.7699, 1.0441

D.2.   Digital simulation

The procedure followed in section 2.1.2 is adopted for the system of Fig. 13. The system of Fig. 13 is equivalently presented as shown in Fig. 15a, b for the Example 6. Subsequently, the digital equivalent is shown in Fig. 15c. The results of digital simulations are shown in Fig. 16a, b, c and d and compared in Table 11 with that of graphical method as well as with the use of MATLAB/SIMULINK.

D.3.   Simulation using Matlab/Simulink

The results of example 6 using MATLAB/SIMULINK are shown in Fig. 16a, b, c and d and the same are compared with that of other methods in Table 11.

Table 11: Comparison of results of Example 6

Method of computation	ω (rad/sec)	X_1	X_2	C_1	C_2
Graphical (phasor Diagram)	0.750	2.074	1.891	1.738	0.469
Digital Simulation	0.740	2.106	1.896	1.773	0.542
SIMULINK	0.748	2.110	1.879	1.754	0.545

www.czasopisma.pan.pl   PAN   www.journals.pan.pl
POLSKA AKADEMIA NAUK

INVESTIGATION OF LIMIT CYCLES AND SIGNAL STABILIZATION
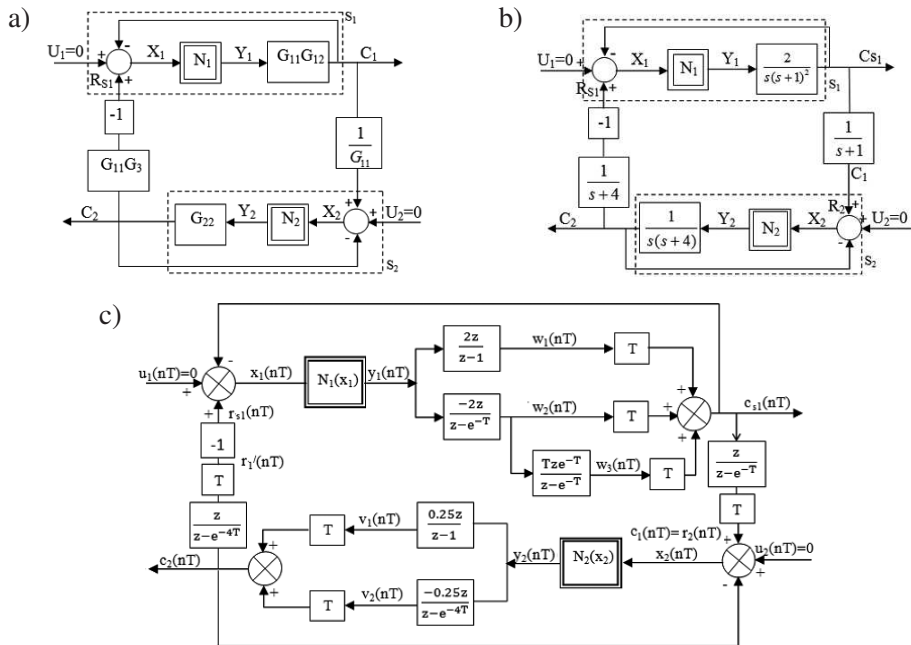OF TWO DIMENSIONAL SYSTEMS WITH MEMORY TYPE NONLINEAR ELEMENTS   317

Figure 15: Digital simulation of the general 2×2 nonlinear system: a) equivalent of Fig. 13, b) equivalent for Example 6, c) digital representation of Example 6 in Z-domain
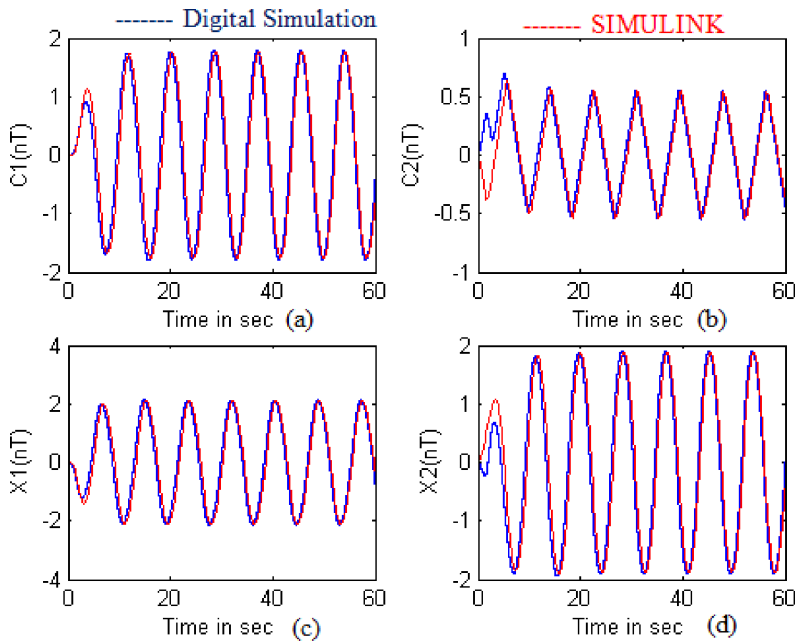

Figure 16: Results obtained for limit cycles (LC) of Example 6 by digital simulations and MATLAB/SIMULINK for general 2×2 nonlinear systems

D.4. Signal stabilization for general 2×2 nonlinear system

In the line of section 3 the general 2×2 system shown in Fig. 13 is examined for signal stabilization, taking $B \sin \omega_f t$ at u_1 point. The procedure depicted in section 2.1.2 is followed for the Example 6 using digital simulations. The results from the digital simulation are shown in Tables 12, 13. During the process of sig-

Table 12: Results of digital simulation for Example 6 showing Synchronization

B	C_1	C_2	ω	Remarks
0.0	1.805	0.554	0.7357	
0.5	1.161	0.471	0.8887	
1.0	0.287	0.544	0.7570	
1.5	0.297	0.667	0.6166	
2.0	0.229	0.710	0.5983	
2.5	0.222	0.719	0.5691	
3.0	0.075	0.587	0.7197	
3.1	0.071	0.601	0.6792	
3.2	0.044	0.557	0.7306	
3.3	0.044	0.557	0.7331	
3.4	0.040	0.552	0.7757	
3.5	0.023	0.497	7.9534	Synchronization
4.0	0.023	0.565	7.9534	

Table 13: Results of digital simulation for Example 6 showing Desynchronization

B	C_1	C_2	ω	Remarks
3.5	0.023	0.497	0.7662	
3.0	0.075	0.587	0.7222	
2.5	0.222	0.719	0.5691	
2.0	0.229	0.710	0.5856	
1.5	0.297	0.664	0.6148	
1.4	0.308	0.634	0.6613	
1.3	0.278	0.613	0.6662	
1.2	0.299	0.613	0.6756	
1.1	0.285	0.587	0.6912	
1.0	0.287	0.547	0.7409	Desynchronization
0.5	1.150	0.471	0.8837	
0.0	1.812	0.555	0.7357	

www.czasopisma.pan.pl   PAN   www.journals.pan.pl
POLSKA AKADEMIA NAUK

INVESTIGATION OF LIMIT CYCLES AND SIGNAL STABILIZATION
OF TWO DIMENSIONAL SYSTEMS WITH MEMORY TYPE NONLINEAR ELEMENTS   319

nal stabilization, the variation of amplitudes C_1, C_2 and frequency ω are shown in Fig. 17a and b respectively. The value of C_1 synchronised with the forcing frequency is clearly shown in Fig. 17c.
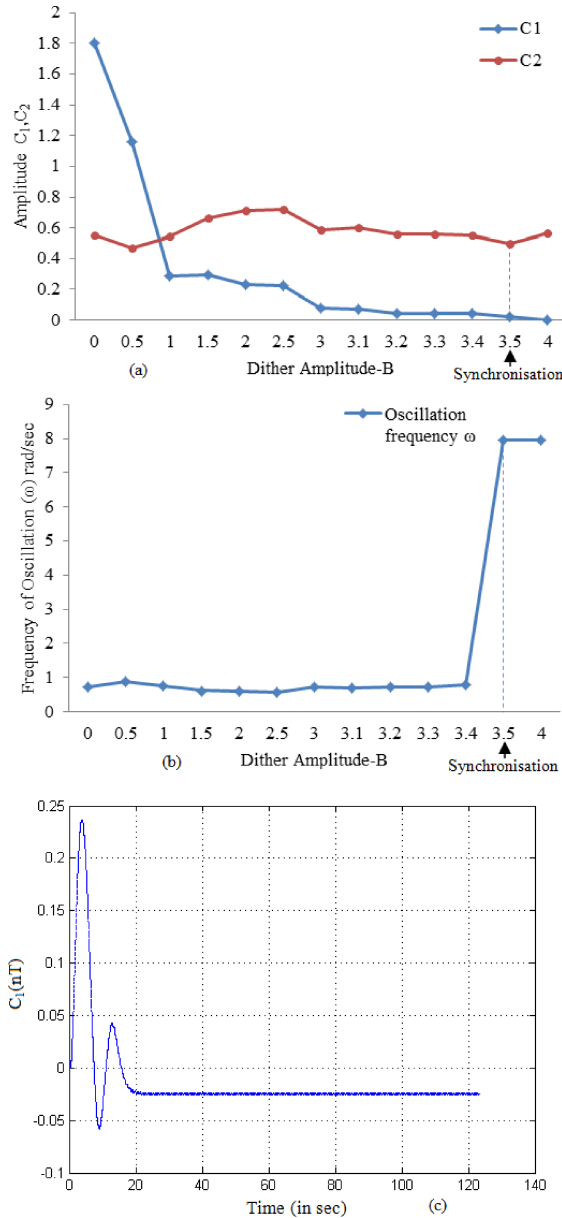
Figure 17: Results of Example 6 of the most general 2×2 systems for signal stabilization: a) variation of C_1 and C_2 with Dither amplitude B, b) variation of ω Dither amplitude B, c) The value of C_1 synchronised with Forcing frequency

E. Conclusion

The graphical procedure illustrated through examples provides a clear insight into the prediction of limit cycle and its quenching by way of signal stabilization for general 2×2 systems with memory type nonlinearities. This is the novelty of the present work which has not been addressed in detail elsewhere. The procedure for determining stability boundary provides a clear and simple method of predicting the existence of limit cycle. This may be much useful for interconnected power system where the governor possesses backlash nonlinearities for selecting a safer zone of operation avoiding such Limit Cycles. The results so obtained are compared with that of digital simulation and also by use of MATLAB/SIMULINK, which substantiates the accuracy of the method and thus claims to be a powerful method to solve such problems.

Appendix A1

Derivation of Describing Function for Backlash type nonlinear elements:

For $X_m > H = \dfrac{b}{2}$ or $X_m > \dfrac{b}{2}$

where β:

$$X_m \sin \beta = X_m - 2H$$

or

$$\beta = \sin^{-1}\left(1 - \frac{2H}{X_m}\right).$$

Equation to output of nonlinear element:

$$y = \begin{cases} K\left(x - \dfrac{b}{2}\right); & 0 \leqslant \omega t \leqslant \dfrac{\pi}{2}, \\ K\left(X_m - \dfrac{b}{2}\right); & \dfrac{\pi}{2} \leqslant \omega t \leqslant (\pi - \beta), \\ K\left(x + \dfrac{b}{2}\right); & (\pi - \beta) \leqslant \omega t \leqslant 3\dfrac{\pi}{2}, \\ K(X_m - H); & \dfrac{3\pi}{2} \leqslant \omega t < (2\pi - \beta), \\ K\left(x - \dfrac{b}{2}\right); & (2\pi - \beta) \leqslant \omega t \leqslant 2\pi. \end{cases}$$

The output is a periodic function but does not possess odd symmetry of nonlinear element but odd half wave symmetry i.e. $y(\omega t \pm \pi) = -y(\omega t)$.

www.czasopisma.pan.pl PAN www.journals.pan.pl
POLSKA AKADEMIA NAUK

INVESTIGATION OF LIMIT CYCLES AND SIGNAL STABILIZATION
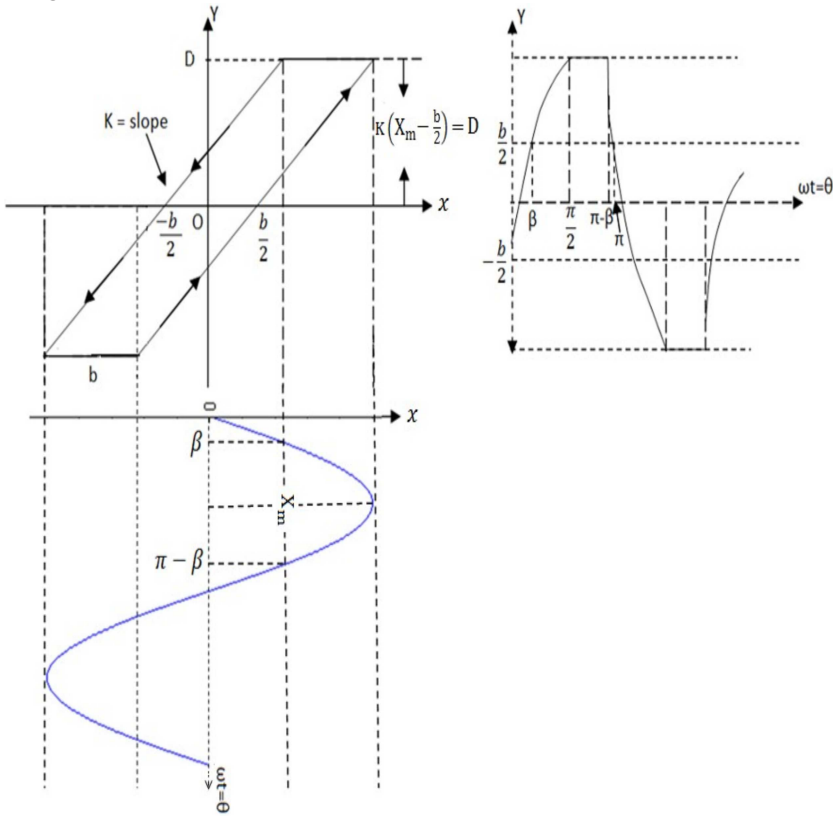OF TWO DIMENSIONAL SYSTEMS WITH MEMORY TYPE NONLINEAR ELEMENTS   321

Consider Fig. 18,

Figure 18: Backlash type nonlinearities (used for derivation of describing function

Therefore, the fundamental component of y is given by:

$$y_1 = A_1 \cos \omega t + B_1 \sin \omega t,$$

where

$$A_1 = \frac{1}{\pi} \int_0^{2\pi} y \cos \omega t \, \mathrm{d}(\omega t)$$

and

$$B_1 = \frac{1}{\pi} \int_0^{2\pi} y \sin \omega t \, \mathrm{d}(\omega t).$$

Due to symmetry of y only the positive half wave need to be considered.

$$
A_1 = \frac{2}{\pi} \left[\int_0^{\pi/2} K(X_m \sin \omega t - H) \cos \omega t \, \mathrm{d}(\omega t) \right.
$$

$$
\left. + \int_{\pi/2}^{\pi-\beta} K(X_m - H) \cos \omega t \, \mathrm{d}(\omega t) + \int_{\pi-\beta}^{\pi} K(X_m \sin \omega t + H) \cos \omega t \, \mathrm{d}(\omega t) \right]
$$

$$
= \frac{2}{\pi} \left[\int_0^{\pi/2} KX_m \sin \theta \cos \theta \, \mathrm{d}\theta - KH \int_0^{\pi/2} \cos \theta \, \mathrm{d}\theta \right.
$$

$$
\left. + K \int_{\pi/2}^{\pi-\beta} (X_m - H) \cos \theta \, \mathrm{d}\theta + \int_{\pi-\beta}^{\pi} KX_m \sin \theta \cos \theta \, \mathrm{d}\theta + KH \int_{\pi-\beta}^{\pi} \cos \theta \, \mathrm{d}\theta \right],
$$

where $\omega t = \theta$

$$
= \frac{2KX_m}{\pi} \left[\int_0^{\pi/2} \left(\frac{\sin 2\theta}{2} \right) \mathrm{d}\theta \right] - \frac{2KH}{\pi} [\sin \theta]_0^{\pi/2}
$$

$$
+ \frac{2K(X_m - H)}{\pi} [\sin \theta]_{\pi/2}^{\pi-\beta} + \frac{2KX_m}{\pi} \left[\int_{\pi-\beta}^{\pi} \left(\frac{\sin 2\theta}{2} \right) \mathrm{d}\theta \right] - \frac{2KH}{\pi} [\sin \theta]_{\pi-\beta}^{\pi}
$$

$$
= \frac{2KX_m}{\pi} \left[-\frac{\cos 2\theta}{4} \right]_0^{\pi/2} - \frac{2KH}{\pi} [1 - 0] + \frac{2K(X_m - H)}{\pi} [\sin \beta - 1]
$$

$$
+ \frac{2KX_m}{\pi} \left[-\frac{\cos 2\theta}{4} \right]_{\pi-\beta}^{\pi} + \frac{2KH}{\pi} [0 - \sin \beta]
$$

$$
= \frac{KX_m}{2\pi} [1 + 1] - \frac{2KH}{\pi} + \frac{2K(X_m - H)}{\pi} \sin \beta - \frac{2K(X_m - H)}{\pi}
$$

$$
+ \frac{2KX_m}{4\pi} [-1 + \cos 2(\pi - \beta)] - \frac{2KH \sin \beta}{\pi}
$$

$$
= \frac{KX_m}{\pi} - \frac{2KH}{\pi} + \frac{2KX_m \sin \beta}{\pi} - \frac{2KH}{\pi} \sin \beta - \frac{2KX_m}{\pi}
$$

$$
+ \frac{2KH}{\pi} - \frac{KX_m}{2\pi} + \frac{KX_m}{2\pi} \cos(2\pi - 2\beta) - \frac{2KH \sin \beta}{\pi}
$$

$$= \frac{KX_m}{2\pi} + \frac{2KX_m \sin\beta}{\pi} - \frac{2KX_m}{\pi} + \frac{KX_m}{2\pi}\cos 2\beta - \frac{4KH}{\pi}\sin\beta$$

$$= \frac{KX_m}{2\pi}[1 + \cos 2\beta] + \frac{2KX_m}{\pi}[\sin\beta - 1] - \frac{4KH}{\pi}\sin\beta$$

$$= \frac{KX_m}{2\pi}2\cos^2\beta + \frac{2KX_m}{\pi}[\sin\beta - 1] - \frac{4KH}{X}\sin\beta$$

$$= \frac{KX_m}{\pi}\cos^2\beta + \frac{2KX_m}{\pi}\left[-1 + \sin\beta\left(1 - \frac{2H}{X}\right)\right]$$

$$= \frac{KX_m}{\pi}\cos^2\beta + \frac{2KX_m}{\pi}[-1 + \sin\beta\sin\beta]$$

or

$$A_1 = \frac{KX_m}{\pi}\cos^2\beta + \frac{2KX_m}{\pi}[-1 + \sin^2\beta] = \frac{KX_m}{\pi}\cos^2\beta + \frac{2KX_m}{\pi}[-1 + 1 - \cos^2\beta]$$

$$= \frac{KX_m}{\pi}\cos^2\beta(1 - 2) = \frac{-KX_m}{\pi}\cos^2\beta. \tag{36}$$

Similarly,

$$B_1 = \frac{2}{\pi}\left[\int_0^{\pi/2} K(X_m\sin\omega t - H)\sin\omega t\, \mathrm{d}(\omega t) + \int_{\pi/2}^{\pi-\beta} K(X_m - H)\sin\omega t\, \mathrm{d}(\omega t)\right.$$

$$\left. + \int_{\pi-\beta}^{\pi} K(X_m\sin\omega t + H)\sin\omega t\, \mathrm{d}(\omega t)\right]$$

$$= \frac{2KX_m}{\pi}\int_0^{\pi/2}\sin\theta.\sin\theta\, \mathrm{d}\theta - \frac{2KH}{\pi}\int_0^{\pi/2}\sin\theta\, \mathrm{d}\theta + \frac{2K(X_m - H)}{\pi}\int_{\pi/2}^{\pi-\beta}\sin\theta\, \mathrm{d}\theta$$

$$+ \frac{2KX_m}{\pi}\int_{\pi-\beta}^{\pi}\sin\theta\sin\theta\, \mathrm{d}\theta + \frac{2KH}{\pi}\int_{\pi-\beta}^{\pi}\sin\theta\, \mathrm{d}\theta$$

$$= \frac{2KX_m}{\pi}\int_0^{\pi/2}\frac{(1 - \cos 2\theta)}{2}\, \mathrm{d}\theta + \frac{2KH}{\pi}[\cos\theta]_0^{\pi/2} - \frac{2K(X_m - H)}{\pi}[\cos\theta]_{\pi/2}^{\pi-\beta}$$

$$+\frac{2KX_m}{\pi}\int\limits_{\pi-\beta}^{\pi}\frac{(1-\cos 2\theta)}{2}-\frac{2KH}{\pi}[\cos\theta]_{\pi-\beta}^{\pi}$$

$$=\frac{2KX_m}{2\pi}\left[\theta-\frac{\sin 2\theta}{2}\right]_0^{\pi/2}+\frac{2KH}{\pi}[0-1]-\frac{2K(X_m-H)}{\pi}[\cos(\pi-\beta)-0]$$

$$+\frac{2KX_m}{2\pi}\left[\theta-\frac{\sin 2\theta}{2}\right]_{\pi-\beta}^{\pi}-\frac{2KH}{\pi}[-1-\cos(\pi-\beta)]$$

$$=\frac{KX_m}{2}-\frac{2KH}{\pi}+\frac{2KX_m}{\pi}\cos\beta-\frac{2KH}{\pi}\cos\beta+KX_m+\frac{KX_m}{2\pi}\sin(2\pi-2\beta)$$

$$-\frac{KX_m}{\pi}(\pi-\beta)+\frac{2KH}{\pi}-\frac{2KH}{\pi}\cos\beta$$

$$=\frac{KX_m}{\pi}\left[\frac{\pi}{2}-0-0\right]-\frac{2KH}{\pi}-\frac{2K(X_m-H)}{\pi}(-\cos\beta)$$

$$+\frac{KX_m}{\pi}\left[\pi+\frac{1}{2}\sin 2(\pi-\beta)-(\pi-\beta)\right]+\frac{2KH}{\pi}-\frac{2KH}{\pi}\cos\beta$$

$$=\frac{3}{2}KX_m+\frac{2KX_m}{\pi}\cos\beta-\frac{2KH}{\pi}\cos\beta-KX_m+\frac{KX_m}{\pi}\beta-\frac{KX_m}{2\pi}\sin 2\beta-\frac{2KH}{\pi}\cos\beta$$

$$=\frac{KX_m}{2}+\frac{2K}{\pi}(X_m-2H)\cos\beta+\frac{KX_m}{\pi}\beta-\frac{KX_m}{2\pi}\sin 2\beta$$

or

$$B_1=\frac{KX_m}{2}+\frac{2K}{\pi}(X_m\sin\beta)\cos\beta+\frac{KX_m}{\pi}\beta-\frac{KX_m}{2\pi}\sin 2\beta\quad(\because X_m-2H=X_m\sin\beta)$$

$$=\frac{KX_m}{2}+\frac{KX_m}{\pi}\sin 2\beta+\frac{KX_m}{\pi}\beta-\frac{KX_m}{2\pi}\sin 2\beta$$

$$=\frac{KX_m}{\pi}+\left[\frac{\pi}{2}+\beta+\sin 2\beta\left(1-\frac{1}{2}\right)\right]=\frac{KX_m}{\pi}\left[\frac{\pi}{2}+\beta+\frac{\sin 2\beta}{2}\right]. \tag{37}$$

Now

$$\text{D.F}=\frac{1}{X_m}[B_1+jA_1]$$

$$=\frac{KX_m}{\pi X_m}\sqrt{\left[\left\{\frac{\pi}{2}+\beta+\frac{1}{2}\sin 2\beta\right\}^2+\{-\cos^2\beta\}^2\right]},$$

$$\theta=\tan^{-1}\frac{A_1}{B_1},$$

where A_1 is $-ve$.

www.czasopisma.pan.pl   PAN   www.journals.pan.pl
POLSKA AKADEMIA NAUK

INVESTIGATION OF LIMIT CYCLES AND SIGNAL STABILIZATION
OF TWO DIMENSIONAL SYSTEMS WITH MEMORY TYPE NONLINEAR ELEMENTS   325

Appendix A2

For $X > \dfrac{b}{2}$

Incremental Input Describing Function (IDF) for backlash nonlinearity:

The IDF for the Backlash nonlinearity [Singh (1968)] can be obtained utilizing the centre and radius of the circle:

The centre of the circle at

$$\left(A + \frac{1}{2}\frac{dA}{dX}\right) + j\left(\beta + \frac{1}{2}\frac{dB}{dX}\right);$$

the radius of the circle is

$$\frac{1}{2}\left\{\left(\frac{dA}{dX}\right)^2 + \left(\frac{dB}{dX}\right)^2\right\}^{\frac{1}{2}},$$

where

$$A = \frac{K}{\pi}\left(\frac{\pi}{2} + \beta + \frac{1}{2}\sin 2\beta\right),$$

$$B = \frac{-K}{\pi}\cos^2\beta,$$

$$\beta = \sin^{-1}\left(1 - \frac{b}{X}\right),$$

$$\left(A + \frac{1}{2}\frac{dA}{dX}\right) = \frac{K}{\pi}\left(\frac{\pi}{2} + \beta + \cos\beta\right),$$

$$\left(B + \frac{1}{2}\frac{dB}{dX}\right) = -\frac{K}{\pi}\frac{b}{X}.$$

For non integral values on n, the IDF is real and is given by $N_i = K$, the slope of backlash nonlinearity for $X > \dfrac{b}{2}$.

Appendix A3

Determination of stability boundary of Example 2:

Consider the Eq. (22) and applying Routh-Hurwitz criterion:

| s^5 | 1 | $(9 + K_2)$ | $(8K_1 + K_2)$ |

$$s^4 \qquad 6 \quad (4+2K_1+2K_2) \quad (4K_1K_2)$$

$$s^3 \quad \frac{6(9+K_2)-(4+2K_1+2K_2)}{6}=a\frac{6(8K_1+K_2)-4K_1K_2}{6}=b$$

$$s^2 \quad \frac{a(4+2K_1+2K_2)-6b}{a}=c \quad 4K_1K_2$$

$$s^1 \quad \frac{bc-a(4K_1K_2)}{c}$$

$$s^0 \quad 4K_1K_2$$

For s^0 row:

$$4K_1K_2 \geqslant 0$$

This implies K_1 and K_2 are positive.

For s^3 row:

$$\frac{6(9+K_2)-(4+2K_1+2K_2)}{6} \geqslant 0 \tag{38}$$

$$\text{ie.} \qquad K_1-2K_2 \geqslant 25.$$

For s^2 row:

$$\frac{a(4+2K_1+2K_2)-6b}{a} \geqslant 0 \quad \text{or}$$

$$\left[\frac{6(9+K_2)-(4+2K_1+2K_2)}{6}\right](4+2K_1+2K_2)$$

$$-6\left[\frac{6(8K_1+K_2)-4K_1K_2}{6}\right] \geqslant 0 \tag{39}$$

$$\text{i.e.} \quad K_1^2-2K_2^2+49K_1-20K_2-7K_1K_2-50 \geqslant 0.$$

For s^1 row:

$$\frac{bc-a(4K_1K_2)}{c} \geqslant 0 \qquad \text{or} \qquad bc-a(4K_1K_2) \geqslant 0 \tag{40}$$

or

$$\left(\frac{48K_1+6K_2-4K_1K_2}{6}\right)\left(\frac{-4K_1^2+8K_2^2-196K_1+80K_2+28K_1K_2+200}{-2K_1+4K_2+50}\right)$$

$$-\frac{(-2K_1+4K_2+50)(4K_1K_2)}{6} \geqslant 0$$

www.czasopisma.pan.pl   PAN   www.journals.pan.pl
POLSKA AKADEMIA NAUK

INVESTIGATION OF LIMIT CYCLES AND SIGNAL STABILIZATION
OF TWO DIMENSIONAL SYSTEMS WITH MEMORY TYPE NONLINEAR ELEMENTS   327

i.e.

$$K_1^3(-192) + K_2^3(-96K_1 + 48) + K_1^2(2904K_2 - 9408)$$
$$+ K_2^2(-1368K_1 + 480) + K_1^2 K_2^2(-48) + K_1 K_2(-8136)$$
$$+ 9600K_1 + 1200K_2 \geqslant 0. \qquad (41)$$

References

[1] D.P. ATHERTON: *Nonlinear control engineering-describing function analysis and design*, VanNostrand Reingold, London, 1975.

[2] D.P. ATHERTON and H.T. DORRAH: A survey on nonlinear oscillations, *International Journal of Control*, **31**(6), (1980), 1041–1105.

[3] I.A. CHIDAMBARAM and S. VELUSAMI: Decentralized biased controllers for load – frequency control of inter connected power systems considering governor dead band non – linearity, In: INDICON, 2005, Annual IEEE, (2005), 521–525.

[4] M. EFTEKHARI and S.D. KATEBI: Evolutionary search for limit cycle and controller design in multivariable nonlinear systems, *Asian Journal of Control*, **8**(4), (2006), 345–358.

[5] O.R. FENDRICH: Describing functions and limit cycles, *IEEE Transactions On Automatic Control*, **37**(4), (1992), 486–487.

[6] A. GELB and W.E. VANDER VELDE: *Multiple-input describing functions and nonlinear system design*, McGraw-Hill, New York. 1968.

[7] R. HAYES and S.P. MARQUES: Prediction of limit cycle oscillations under uncertainty using a Harmonic Balance Method, Elsevier, *Computers and Structures*, **148**, (2015), 1–13.

[8] D. IURASHEV, G. CAMPA, V.V. ANISIMOV, and E. COSATTO: Three-step approach for prediction of limit cycles pressure oscillations in combustion chambers of gas turbines, Taylor and Fransis, *Combustion Theory and Modelling*, **21**(6), (2017), 1–28.

[9] V. JAIN, D. GARG, and A.K. ARORA: Digital Simulation of Limit Cycle in Second and Higher Order Analog Filter using MATLAB, *International Journal of Computer Applications*, **53**(2), (2012), 29–32.

[10] M. KATEBI, H. TAWFIK and S.D. KATEBI: Limit Cycle Prediction Based on Evolutionary Multi-objective Formulation, *Mathematical Problems in Engineering*, (2009), 1–17.

[11] J. LI, Y. XIA, A.S. MORGANS, and X. HAN: Numerical prediction of combustion instability limit cycle oscillations for a combustor with a long flame, Elsevier, Combustion and flame, 185, (2017), 28–43.

[12] L.H. LIM and *A.P. Loh*: Forced and sub- harmonic oscillations in relay feedback systems, *Journal of the Institution of Engineers Singapore*, **45**(5), (2005), 88–100.

[13] C.H. LIN and K.W. HAN: Prediction of limit- cycles in nonlinear two-input two-output control systems, *IEE Proceedings-Control Theory and Applications*, **146**(3), (1999), 253–258.

[14] A.P. LOH and V.U. VASNANI: Necessary conditions for limit cycles in multi loop relay systems, *IEE Proceedings-Control Theory and Applications*, **141**(3), (1994), 163–168.

[15] C.F. LU, C.C. LIU, and C.J. WU: Effect of battery energy storage system on load frequency control considering governor dead band and generation rate constraint, *IEEE Transactions energy Conversions*, **10**(1), (1995), 555–561.

[16] P.N. NIKIFORUK and B.L.M. WINTONYK: Frequency response analysis of two-dimensional nonlinear symmetrical and non symmetrical control systems, *Int. J. Control*, **7**, (1968), 49–62.

[17] R. OLDENBURGER and T. NAKADA: Signal stabilization of self-oscillating systems, *IRE Transactions on Automatic Control*, **6**(3), (1961), 319–325.

[18] A.G. PARLOS, A.F. HENRY, F.C. SCHWEPPE, L.A. GOULD, and D.D. LANNING: Nonlinear multivariable control of nuclear power plants based on the unknown-but-bounded disturbance model, *IEEE Transactions on Automatic Control*, **33**(2), (1988), 130–137.

[19] B.B. PATI and K.C. PATRA: Normalised phasor Diagram Method of Prediction of Limit Cycle for Two-dimensional Nonlinear System, *Journal – Institution of Engineers India Part Electrical Engineering Division*, (2000), 140–144.

[20] B.B. PATI and K.C. PATRA: Dither in Two- dimensional System with Memory less Non- linearity and System Stability, *Journal – Institution of Engineers India Part Electrical Engineering Division*, **84**, (2004), 173–177.

[21] K.C. PATRA: Analysis of self-oscillations and signal stabilisation of two-dimensional nonlinear systems, Ph.D. Thesis, Electrical Engg, IIT Kharagpur, India (1986).

[22] K.C. PATRA and B.B. PATI: An investigation of forced oscillation for signal stabilisation of two-dimensional nonlinear system, *Systems and Control Letters*, **35**(4), (1998), 229–236.

[23] K.C. PATRA, B.B. PATI, and J. KACPRZYK: Prediction of limit cycles in nonlinear multivariable systems, *Archives of Control Science*, **4**, (1995), 281–298.

[24] K.C. PATRA, B.B. PATI, and J. KACPRZYK: Signal stabilisation of two dimensional non linear relay control systems, *Archives of Control Science*, **6**, (1997), 89–102.

[25] K.C. PATRA and Y.P. SINGH: Structural formulation and prediction of limit cycle for multivariable nonlinear system, *IETE Journal of Research*, **40**(5-6), (1994), 253–260.

[26] K.C. PATRA and Y.P. SINGH: Graphical method of prediction of limit cycle for multivariable nonlinear systems, *IEE Proceedings-Control Theory and Applications*, **143**(5), (1996), 423–428.

[27] P.K. RAJAGOPALAN and J. MISHRA: Dual-input describing function of double-valued nonlinearities, In Proceedings of the Institution of Electrical Engineers, *IET*, **116**(10), (1969, October), 1764–1768.

[28] P.K. RAJAGOPALAN and Y.P. SINGH: Analysis of harmonics and almost periodic oscillations in forced self-oscillating systems, In Proc. 4th IFAC Congress, Warsaw, **41**, (1969), 80–122.

[29] G.V.S. RAJU and R. JOSSELSON: Stability of reactor control systems in coupled core reactors. IEEE Transactions on Nuclear Science, 18(1), (1971). 388-394.

[30] Z. SHI and Z. ZUO: Backstepping control for gear transmission servo systems with backlash nonlinearity, *IEEE Trans. Autom. Sci. Eng.*, **12**(2), (2015), 752–757.

[31] Y.P. SINGH: Some aspects of forced oscillations of non-linear systems (Doctoral dissertation, Ph. D. Thesis, Electrical Engg, IIT Kharagpur, India. (1968).

[32] T.S. TSAY: Load-frequency control of inter connected power system with governor backlash nonlinearities, *Electrical Power and Energy Systems*, **33**, (2011), 1542–1549.

[33] T.S. TSAY: Limit cycle predictions of nonlinear multivariable feedback control systems with large transportation lags. *Journal of Control Science and Engineering*, **7**, (2011), 1–11.

[34] T.S. TSAY: Stability analyses of nonlinear multivariable feedback control systems, *WSEAS Transactions on Systems*, **11**(4), (2012), 140–151.

[35] S.C. TRIPATHY, G.S. HOP, and O.P. MALIK: Optimisation of Load-frequency control parameters for power system with read steam turbines and governor dead band nonlinearity, *PROC IEE. Ptc*, **129**(1), (1982), 10–16.

[36] C. WANG, M. YANG, W. ZHENG, K. HU, and D. XU: Analysis and Suppression of Limit Cycle Oscillation for Transmission System With Backlash Nonlinearity, *IEEE transactions on Industrial Electronics*, **64**(12), (2017), 9261–9270.

[37] M. ZHUANG and D.P. ATHERTON: PID controller design for a TITO system, *IEE Proceedings-Control theory and applications*, **141**(2), (1994), 111–120.